



Application of Simplified Energy Concept for Liquefaction Prediction in Bengkulu City, Indonesia

Lindung Zalbuin Mase[✉] · Sintia Agustina · Hardiansyah ·
Muchammad Farid · Fepy Supriani · Weeradeth Tanapalungkorn ·
Suched Likitlersuang

Received: 2 November 2022 / Accepted: 4 February 2023 / Published online: 22 February 2023
© The Author(s), under exclusive licence to Springer Nature Switzerland AG 2023

Abstract This work presents an application of a simplified energy concept for predicting liquefaction potential based on data collected during the M_w 8.6 Bengkulu-Mentawai Earthquake in Bengkulu, City, Indonesia. A total of 38 sites are investigated through seismic data and soil characteristics. One dimensional seismic response analysis is then conducted to determine the peak ground acceleration within each soil layer of the study area. From the peak ground acceleration values, kinetic velocity values are generated. The maximum kinetic energy density due to earthquake shaking is determined using the simplified energy concept. The Empirical analysis is employed to predict liquefaction potential. The empirical analysis results are then correlated to kinetic energy density to generate equations that estimate liquefaction potential in Bengkulu City. Results show that a simplified

energy concept can be used to estimate liquefaction potential. The performance of the proposed equations is generally consistent with documented liquefaction cases from around the world, and thus the framework implemented in this study can be adopted to calculate liquefaction potentials in other areas worldwide.

Keywords Bengkulu city · Earthquake · Liquefaction · Simplified energy · Seismic ground response

1 Introduction

Earthquakes can occur due to several tectonic activities (Dong and Luo 2022). Earthquake mechanisms and effects had been intensively discussed in Geosciences, Seismology, and Engineering (Dong and Luo 2022; Mase 2021; Mase et al. 2022b). Bengkulu City is an earthquake-prone area in Indonesia (Mase 2020). Two large earthquakes have occurred in Bengkulu City (Mase 2018a): the M_w 7.9 Bengkulu-Enggano Earthquake in 2000 (Farid and Mase 2020), and the M_w 8.6 Bengkulu-Mentawai Earthquake in 2007 (Mase 2021). The M_w 8.6 Bengkulu-Mentawai Earthquake in 2007 had also triggered structural damage, such as buildings collapse, infrastructure damage, and public and private facilities damage (Hausler and Anderson 2007). Hausler and Anderson (2007) also recorded that the earthquake also triggered liquefaction in Bengkulu City. Mase (2017) and

L. Z. Mase (✉) · S. Agustina · Hardiansyah · F. Supriani
Department of Civil Engineering, Faculty of Engineering,
University of Bengkulu, Bengkulu, Indonesia
e-mail: lmase@unib.ac.id

M. Farid
Department of Geophysics, Faculty of Mathematics
and Natural Sciences, University of Bengkulu, Bengkulu,
Indonesia

W. Tanapalungkorn · S. Likitlersuang
Centre of Excellence in Geotechnical and Geoenvironmental
Engineering, Department of Civil Engineering, Faculty
of Engineering, Chulalongkorn University, Bangkok,
Thailand

Misliniyati et al. (2018) reported various evidence of liquefaction such as sand boils and lateral spreads found along the coastline of Bengkulu, especially during the M_w 8.6 Bengkulu-Mentawai Earthquake in 2007. Several liquefaction cases from other areas during large earthquakes are also reported by several researchers, such as Sukkarak et al. (2021) during the Tarlay Earthquake on the border of Thailand-Myanmar in 2011, Mase et al. (2021a) during the Yogyakarta Earthquake in Indonesia in 2006, Mase et al. (2022b) during the Kobe Earthquake in Japan in 1995, and Kusumawardani et al. (2021) during the Palu Earthquake in Indonesia in 2018. Therefore, liquefaction during earthquakes is still becoming a hot issue for many researchers of Geotechnical Earthquake Engineering.

Studies about soil liquefaction and earthquake in Bengkulu City are studied in Bengkulu City. Studies conducted by Mase (2017), Mase (2018a), Misliniyati et al. (2018), and Farid and Mase (2020), achieved two main results, i.e., applying field test data and using seismic ground response analysis to depict soil behaviour during earthquakes could be used for estimation liquefaction potential and earthquake impact. However, the study focused on the development of simple charts for engineering practice to predict liquefaction potential in Bengkulu City is still limited. Meanwhile, the prediction of liquefaction potential considering site investigation data and numerical analyses is still limited (Mase et al. 2022a).

Prediction of liquefaction potential has been developed by several researchers. Several liquefaction predictions reflected by the simplified procedure considering site investigation data had been proposed by Robertson and Wride (1998), Andrus et al. (2004), Boulanger and Idriss (2014), and Mase et al. (2020a, b). Generally, those studies estimate cyclic resistance ratio and cyclic stress ratio as determining the factor of safety (FS) which is used as a governing factor of liquefaction potential. Jafarian et al. (2012) mentioned that the prediction of cyclic resistance ratio for liquefiable soils and simplified liquefaction analysis could be also an alternative for seismic design. However, there has been an absence of determining liquefaction potential based on kinetic energy density combined with seismic ground response analysis.

Advances in energy-based liquefaction potential analysis have been presented by several researchers. Initially, Nemat-Nasser and Shokoh (1979)

introduced the energy-based approach as an alternative method to predict liquefaction potential. Then, Berrill and Davis (1985), Figueroa et al. (1994), Kayen and Mitchell (1997), Green and Mitchell (2004), Jafarian et al. (2012), Kokusho (2013), and Azeiteiro et al. (2017) progressively and intensively developed the energy-based liquefaction prediction approach. Generally, the energy-based approach is based on the direct correlation between energy dissipation per unit volume and pore water pressure during cyclic loading (Sonmezer 2019). Jafarian et al. (2008) and Jafarian et al. (2013) determined that kinetic energy can be used as a parameter to estimate liquefaction potential. Amini and Noorzad (2018) stated that the use of the energy-based approach is reasonable since the energy of liquefaction is strongly dependent on the applied shear stress and shear strain. Besides, the implementation of non-linear ground response analysis had been developed in many areas related to earthquake and liquefaction effects. Kundu et al (2021) studied site characterization and liquefaction potential of soils in Northern India. Kundu et al. (2021) also mentioned that based on experimental and numerical analysis, the studied excess pore pressure ratio on the studied site indicates liquefaction. Naik et al. (2022) also mentioned that non-linear ground response analysis had been successfully implemented to observe ground response and liquefaction potential in Himalayan Frontal Thrust. Generally, the implementation of ground response analysis is addressed to observe soil behaviour that indicates liquefaction, such as excess pore water pressure. Meanwhile, the further use of ground response such as layer acceleration due to ground response analysis to predict energy density to trigger liquefaction is still limited to perform. As such, the energy-based model is generally developed from experimental studies (Sonmezer 2019), but it has rarely been implemented in combination with non-linear site response analysis. Therefore, it is important to show the correlation between ground-response analysis and energy-based model for liquefaction prediction.

Seismic ground response analysis combined with a simplified energy concept for predicting liquefaction is still rarely performed. This study presents the application of a simplified energy concept for liquefaction prediction, in Indonesia based on the earthquake event of the Bengkulu Mentawai Earthquake in 2007 (M_w 8.6). First, non-linear ground response

analysis (1D NSRA) is employed to obtain the ground motion parameters of soil layers. Acceleration from 1D NSRA is used to estimate the maximum kinetic energy density (*MKED*). Besides, a semi-empirical procedure analysis based on site investigation data is first performed to obtain a factor of safety against liquefaction (*FS*). The correlations between *MKED*, soil resistance, and *FS* are generated. The models are addressed for determining the liquefaction vulnerability model for engineering practice. The results of this study will be useful for the Indonesian government in their efforts to plan against liquefaction disasters on residential and general infrastructures in Bengkulu City and other neighbour cities.

2 Seismotectonic Settings and Geological Condition of Bengkulu City

The seismotectonic settings of Bengkulu City are illustrated in Fig. 1. Bengkulu City, the capital of Bengkulu Province, is known to be an area of high earthquake risk in Indonesia (Misliniyati et al. 2018).

Bengkulu City is located on the west coast of Sumatra Island, which is also known as a tectonically active region (Fig. 1). Mase (2020) explained that Bengkulu Province is located near the subduction zone between the Indo-Australian plate and the Eurasian plate. The movement generated by the collision of these two plates creates the formation of active faults in the western part of Sumatra, i.e., both Semangko and Mentawai Faults (McCaffrey 2009; Natawidjaja and Triyoso 2007). Some moderate to strong earthquakes such as the Liwa Earthquake in 1996 (Widiwijayanti et al. 1996); the Bengkulu-Mentawai Earthquake in 2007 (Mase 2021), and the Padang Earthquake in 2009 (Wiseman et al. 2012) occurred due to tectonic activity in this tectonic region. For Bengkulu City, the Bengkulu-Mentawai Earthquake in 2007 triggered liquefaction in Bengkulu City, as shown in Fig. 2.

The geological map of Bengkulu City is shown in Fig. 3. There are several geological formations found in Bengkulu City, i.e., Bintunan Formation (QTb), Alluvium (Qa), Reef Limestone (Ql), Alluvium Terraces (Qat), Swamp Deposits (Qs), and Andesite (Tpan) (Natural Disaster Agency 2018). In terms of

Fig. 1 Seismotectonic setting of Bengkulu Province (Modified from Mase 2020)

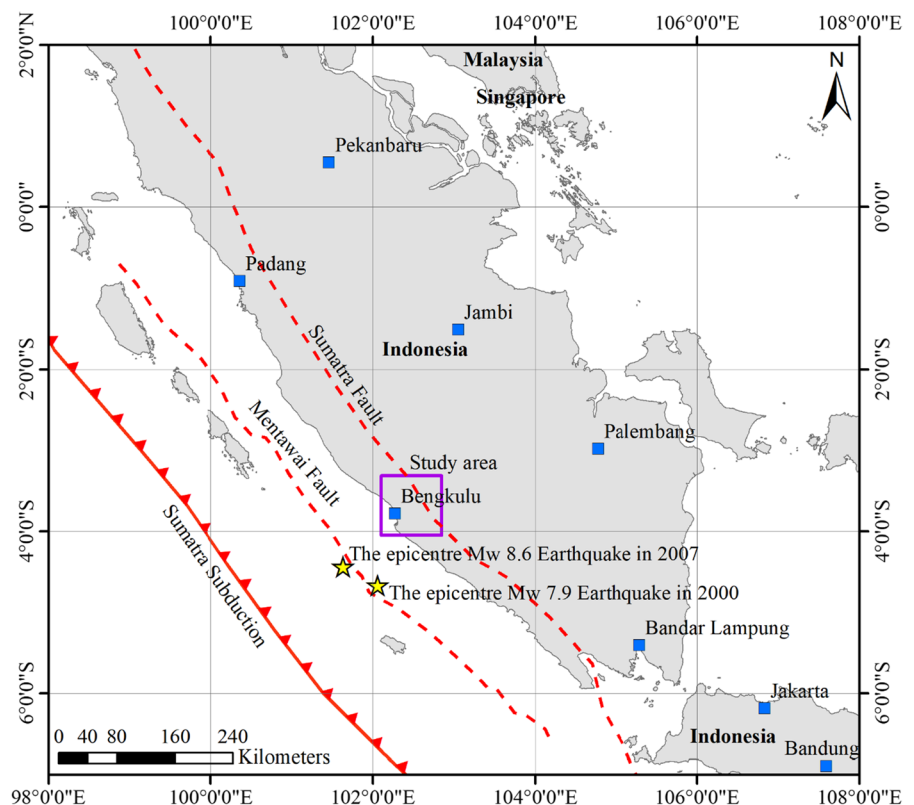
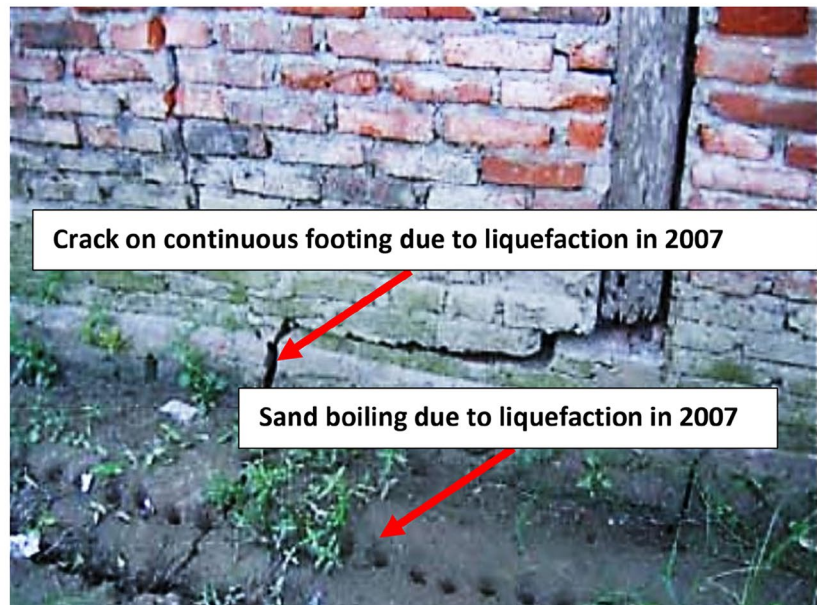


Fig. 2 Liquefaction evidence found during the Mw 8.6 Bengkulu-Mentawai Earthquake in 2007 (Hau-sler and Anderson 2007) **a** large settlement, **b** sand boils manifestation and crack on continuous footing



(a)

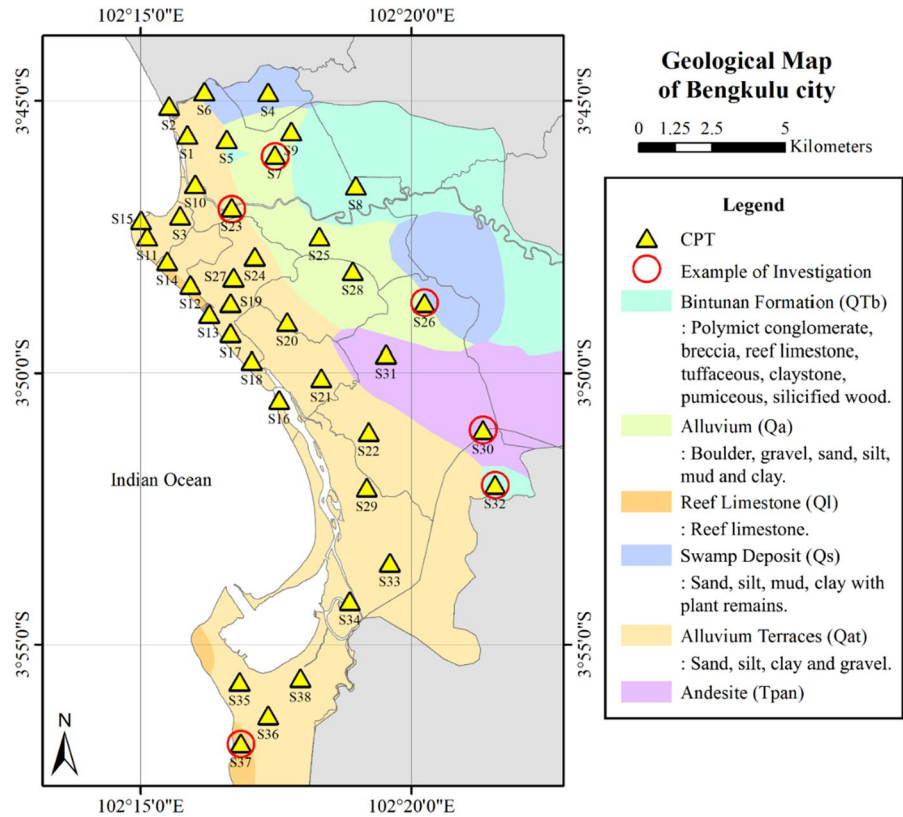


(b)

topographical condition, Bengkulu City can be categorized into three areas, i.e., low terrain, high terrain, and coastal area. In the low terrain and coastal areas (the western part of Bengkulu City), Qat is generally found and dominated by several materials, such as sand, silt, clay, and gravel. For the coastal area, a small zone of Ql is also found. The high terrain area (eastern part) of Bengkulu City is composed of Tpan, Qs, QTb, and Qa; these formations are generally

dominated by high-density sediment and rocks (Mase 2020; Farid and Mase 2020, base 2020). In line with liquefaction in Bengkulu City, Mase (2020, b, 2017) and Farid and Mase (2020) mentioned that Qat formation is relatively more to undergo liquefaction, especially if the formation is located at basin area with shallow groundwater level. Yilmaz et al. (2008) and Sana and Nath (2016) also mentioned that areas such as Beydag (Turkey) and Kashmir valley (Himalaya)

Fig. 3 Geological map of Bengkulu City (Modified from Natural Disaster Agency of Bengkulu Province 2018; Mase 2020)



dominated by alluvium composed by sandy soils are relatively having high liquefaction potential.

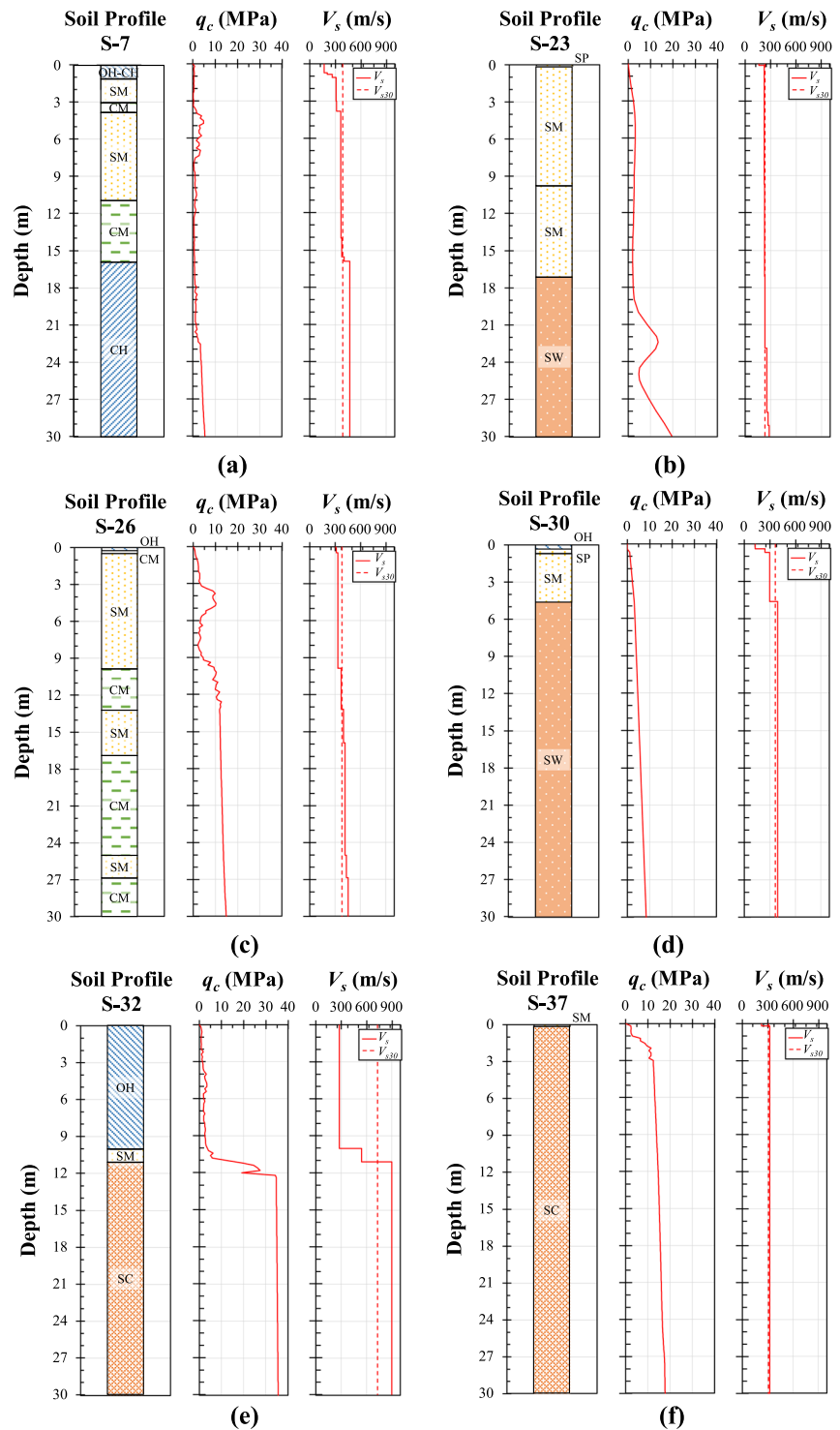
The layout of the site investigation used in this study is also presented in Fig. 3. The site investigation involved collecting data on soil profile and resistance, as well as the shear wave velocity (V_s) from 38 sites. Soil resistances on penetration value and shear wave velocity profile are collected from cone penetration test (CPT) and Multi-Channel Analysis of Surface Waves (MASW) test. The use of CPT has some advantages in geotechnical engineering practice. The cone penetration test gives a continuous record of the penetration resistance with depth and it is less susceptible to operator error than the standard penetration test (Rezania et al. 2010). Liquefaction methods based on the CPT have the advantage of continuous, repeatable measurements but require corrections based on soil characteristics that can be significant in soils with high fine content). Liquefaction methods base on shear wave velocity have the advantage that they are essentially independent of soil characteristics, such as fines content, but often lack the stratigraphic detail obtained using the CPT (Robertson 2015). Therefore,

the combination of those two methods can be resulted a better prediction for liquefaction potential.

Some of the soil-layer interpretation results at the investigation sites are shown in Fig. 4 (these examples reflect the subsoil conditions in several parts of Bengkulu City). S-7, composed of Qa formation, is located in flood-prone areas. S-23 is located in the Qat-composed area, while S-26 is located in the Qs-composed area. S-30, S-32, and S-37 are located in Tpan, QTb, and Ql formations, respectively.

Sites S-23, S-30, and S-37 are mainly composed of sandy soil. At these sites, we found sandy soils classified as poor-graded sand (SP), silty sand (SM), clayey sand, and well-graded sand (SW). In terms of soil resistance, the cone resistances (q_c) of these sites have an average value of about 6 to 12 MPa. Also, the time-averaged shear wave velocity for the first 30 m depth ($V_{s,30}$) was observed to vary from 250 to 375 m/s. Therefore, these sites are classified into Site Class D based on National Earthquake Hazard Reduction Provision (NEHRP) (1998). At sites S-7, S-26, and S-32, thin clay layers inserted in dominant sandy soils were found. In general, these sites have

Fig. 4 Examples of site investigation data in the study area: **a** S-7, **b** S-23, **c** S-26, **d** S-30, **e** S-32, and **f** S-37



an average q_c value of about 5 to 20 MPa, and their V_{s30} values vary from 396 to 745 m/s. The recapitulation of V_{s30} , V_s range, and site class is compiled in

Table 1. Therefore, these sites are classified into Site Classes C. From the site investigation results, it was found that, in general, Bengkulu City is dominated

Table 1 Recapitulation of V_s range, V_{s30} and site class for first 30 m depth

| No | Sites code | Location | | Districts | V_s range (m/s) | V_{s30} (m/s) | Site class |
|----|------------|--------------|---------------|------------------|-------------------|-----------------|------------|
| | | Latitude (°) | Longitude (°) | | | | |
| 1 | S-1 | -3.758 | 102.259 | Muara Bangkahulu | 256–363 | 355 | D |
| 2 | S-2 | -3.743 | 102.252 | Muara Bangkahulu | 304–451 | 352 | D |
| 3 | S-3 | -3.780 | 102.262 | Muara Bangkahulu | 241–299 | 298 | D |
| 4 | S-4 | -3.759 | 102.277 | Muara Bangkahulu | 286–430 | 402 | C |
| 5 | S-5 | -3.766 | 102.271 | Muara Bangkahulu | 151–373 | 331 | D |
| 6 | S-6 | -3.753 | 102.271 | Muara Bangkahulu | 267–357 | 352 | D |
| 7 | S-7 | -3.778 | 102.283 | Muara Bangkahulu | 181–375 | 350 | D |
| 8 | S-8 | -3.751 | 102.292 | Muara Bangkahulu | 227–302 | 299 | D |
| 9 | S-9 | -3.768 | 102.291 | Muara Bangkahulu | 180–375 | 350 | D |
| 10 | S-10 | -3.784 | 102.260 | Teluk Segara | 244–329 | 328 | D |
| 11 | S-11 | -3.789 | 102.250 | Teluk Segara | 154–326 | 291 | D |
| 12 | S-12 | -3.798 | 102.253 | Teluk Segara | 223–355 | 342 | D |
| 13 | S-13 | -3.796 | 102.251 | Teluk Segara | 161–332 | 305 | D |
| 14 | S-14 | -3.798 | 102.255 | Teluk Segara | 163–286 | 270 | D |
| 15 | S-15 | -3.791 | 102.250 | Teluk Segara | 247–295 | 277 | D |
| 16 | S-16 | -3.809 | 102.265 | Ratu Samban | 273–292 | 286 | D |
| 17 | S-17 | -3.811 | 102.267 | Ratu Samban | 202–299 | 298 | D |
| 18 | S-18 | -3.816 | 102.273 | Ratu Samban | 140–323 | 297 | D |
| 19 | S-19 | -3.799 | 102.263 | Ratu Samban | 149–322 | 314 | D |
| 20 | S-20 | -3.818 | 102.276 | Ratu Agung | 229–324 | 324 | D |
| 21 | S-21 | -3.837 | 102.295 | Ratu Agung | 199–463 | 373 | C |
| 22 | S-22 | -3.852 | 102.305 | Ratu Agung | 99–298 | 254 | D |
| 23 | S-23 | -3.797 | 102.283 | Ratu Agung | 114–338 | 295 | D |
| 24 | S-24 | -3.818 | 102.285 | Ratu Agung | 170–469 | 387 | C |
| 25 | S-25 | -3.782 | 102.293 | Sungai Serut | 239–509 | 476 | C |
| 26 | S-26 | -3.790 | 102.326 | Sungai Serut | 197–456 | 394 | C |
| 27 | S-27 | -3.816 | 102.288 | Singaran Pati | 159–283 | 235 | D |
| 28 | S-28 | -3.821 | 102.309 | Gading Cempaka | 127–392 | 364 | C |
| 29 | S-29 | -3.868 | 102.319 | Selebar | 205–371 | 356 | D |
| 30 | S-30 | -3.850 | 102.350 | Selebar | 126–572 | 437 | C |
| 31 | S-31 | -3.837 | 102.322 | Selebar | 166–351 | 334 | D |
| 32 | S-32 | -3.880 | 102.353 | Selebar | 234–645 | 458 | C |
| 33 | S-33 | -3.890 | 102.322 | Kampung Melayu | 160–398 | 392 | C |
| 34 | S-34 | -3.915 | 102.308 | Kampung Melayu | 308–406 | 437 | C |
| 35 | S-35 | -3.930 | 102.287 | Kampung Melayu | 277–899 | 507 | C |
| 36 | S-36 | -3.938 | 102.284 | Kampung Melayu | 181–477 | 434 | C |
| 37 | S-37 | -3.938 | 102.289 | Kampung Melayu | 277–773 | 606 | C |
| 38 | S-38 | -3.930 | 102.304 | Kampung Melayu | 178–580 | 467 | C |

by granular soils with inserted cohesive soils among sand layers. Mase et al. (2021b) and Mase (2022) also mentioned that Bengkulu City is generally dominated by sandy soils. In their studies, Mase et al. (2021b) and Mase (2022) also presented that there are two

main site classes in Bengkulu City, i.e., Site Classes C and D. Therefore, the results of the site investigation conducted in this study are generally consistent with previous studies. Sites with thick sand layers and low soil resistance tend to have liquefaction potential,

thus the site investigation results confirm the area's liquefaction potential. V_s less than 150 m/s also indicates medium to low-density soils which translate to layers that are prone to liquefaction.

3 Theory and Method

3.1 Non-Linear Seismic Wave Propagation

The non-linear effective stress model proposed by Elgamal et al. (2006) is a frequently used one-dimensional non-linear seismic ground response analysis (1D NSRA) method. 1D NSRA method implemented in this study is addressed to results in ground motion parameters, such as peak ground acceleration for each layer that is used for the semi-empirical analysis of liquefaction potential and the maximum energy density analysis. Misliniyati et al. (2019) showed that this method can obtain results that are relatively consistent with field evidence found during strong earthquakes; therefore, it can be simply noted that this method has previously been reasonably implemented. An overview of the procedures to model seismic wave propagation was provided by Mase et al. (2018) within the context of the 2011 Tarlay earthquake at the Thailand-Myanmar border. First, earthquake waves propagate from the bedrock surface and pass through each soil layer; and although the boundary conditions in 1D modelling are limited to the vertical direction, displacement is still allowed in both the vertical and horizontal bearings. Once the waves propagate, soil behaviour can be interpreted as several relationships, such as ground-motion time history, frequency content, or hysteresis loops. According to Mase (2020),

the depth of engineering bedrock in Bengkulu City is generally found at 30 m depth. Therefore, in this study, the input motion is first applied at the bottom of the soil layer at 30 m depth.

During the Bengkulu Mentawai Earthquake in 2007, there was no actual ground motion was recorded. Therefore, for engineering practice and hazard prediction, synthetic ground motions were generated to generate representative ground motions in the study area during the earthquake. Mase (2018a) mentioned that several ground motions records can be used as representative ground motions for engineering purposes in Bengkulu City; they are the motions of Loma Prieta, Imperial Valley, Kobe, Northridge, and Chichi. According to Mase (2018a), these motions were selected since they consider seismicity factors such as the source mechanism, site area, maximum earthquake magnitude, and so on, which are relevant to Bengkulu City as presented in Table 2. Elsewhere, the development of the local spectral design proposed by Mase and Somantri (2016) suggested an updated procedure for earthquake resistance designs in Bengkulu City. In this study, the ground motion for the input motion is generated based on a spectral matching method (Hancock et al. 2006). The ground motion used in this study is based on Mase and Somantri (2016) who developed the local spectral response for Bengkulu City based on geological conditions, site characteristics, and earthquake mechanisms. From this local spectral response in Bengkulu City, the spectral matching method from Hancock et al. (2006) is implemented to generate artificial ground motion. In this study, the spectral acceleration of the Loma Prieta Earthquake motion is used as the matching spectral acceleration based on the

Table 2 Summary of relevant earthquake characteristics to Bengkulu City based on Mase (2018a)

| Date of event | Earthquake name | Location | Tectonic condition | Site class | Earthquake magnitude (M_w) | Maximum modified Mercalli Intensity |
|--------------------|-------------------|-----------|------------------------|------------|--------------------------------|-------------------------------------|
| October 17, 1989 | Loma Prieta | USA | Active tectonic region | D | 6.9 | X |
| October 15, 1979 | Imperial Valley | USA | Active tectonic region | D | 6.5 | IX |
| January 17, 1995 | Kobe | Japan | Active tectonic region | D | 6.9 | XI |
| January 17, 1995 | Northridge | USA | Active tectonic region | D | 6.7 | IX |
| September 21, 1999 | Chichi | Taiwan | Active tectonic region | D | 7.7 | X |
| September 12, 2007 | Bengkulu-Mentawai | Indonesia | Active tectonic region | D | 8.6 | IX |

recommendation from Mase (2018a). Mase (2018a) mentioned that the Loma Prieta motion tends to result in the highest amplification among all the suggested representative ground motions. Several studies conducted by Bowden and Tsai (2017), Li et al. (2019), Likitlersuang et al. (2020), Sukkarak et al. (2021) and Mase et al. (2021c) have explained that the effect of ground motion amplification can result in strong surface damage. Therefore, it is reasonable to use the motion of the Loma Prieta Earthquake in this study. After matching ground motion, the artificial spectral acceleration processed by the spectral matching method is generated, as shown in Fig. 5. It can be seen that the maximum peak ground acceleration (PGA) was about 0.369 g.

Based on Kramer (1996), a minimum PGA of 0.1 g is required to trigger liquefaction. de Magistris et al. (2013) mentioned that PGA of 0.09 g could be set up as a rational approach for liquefaction threshold. However, this value is very close to the recommendation suggested by National Research Council (NRC 1985). Zhu et al. (2017) also mentioned liquefaction occurrences were consistent with PGA of more than 0.1 g. Therefore, Rashidian and Baise (2020) suggested that PGA of 0.1 g is relevant as liquefaction threshold. The comparison of ground motion parameters between the original motion and input motion is shown in Table 3. The input motion is propagated starting from the bottom of the investigated site. Furthermore, several results, such as

Fig. 5 Spectral matching results to generate input motion for seismic ground response (Raw data from Mase and Somantri 2016) **a** spectral acceleration comparison and **b** comparison of matched motion and input motion

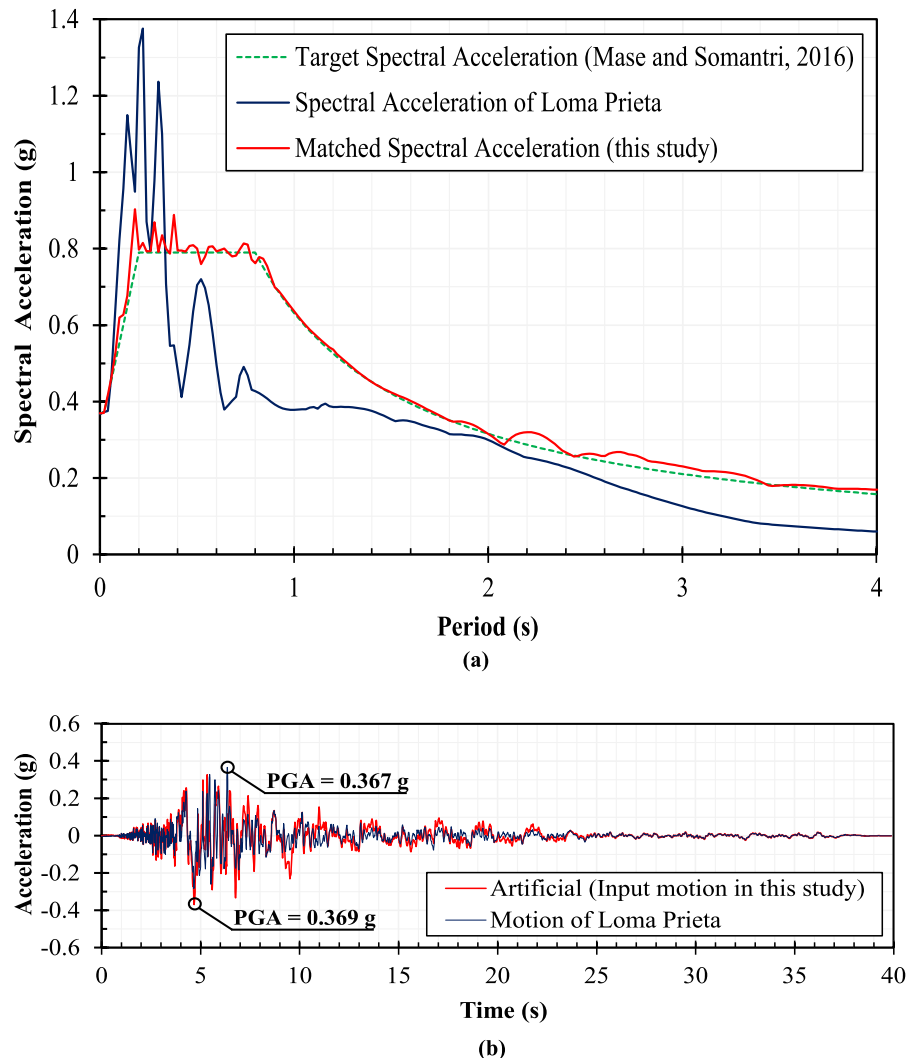


Table 3 Ground motion parameters

| No | Ground motion parameters | Accelerograms | |
|----|--|---------------|----------|
| | | Original | Matched |
| 1 | Maximum acceleration (g) | 0.367 | 0.369 |
| 2 | Maximum velocity (cm/s) | 44.695 | 60.943 |
| 3 | Maximum displacement (cm) | 19.615 | 69.611 |
| 4 | V_{max}/a_{max} (s) | 0.124 | 0.168 |
| 5 | Acceleration RMS (g) | 0.047 | 0.058 |
| 6 | Velocity RMS (cm/s) | 6.796 | 12.239 |
| 7 | Displacement RMS (cm) | 3.467 | 41.058 |
| 8 | Arias intensity | 1.348 | 2.041 |
| 9 | Characteristic intensity | 0.064 | 0.087 |
| 10 | Specific energy density (cm ² /s) | 1843.333 | 5977.814 |
| 11 | Cumulative absolute velocity (cm/s) | 936.569 | 1235.995 |
| 12 | Acceleration spectrum intensity (g s) | 0.338 | 0.317 |
| 13 | Velocity spectrum intensity (cm) | 169.786 | 217.965 |
| 14 | Housner intensity (cm) | 164.939 | 209.114 |
| 15 | Sustained maximum acceleration (g) | 0.301 | 0.327 |
| 16 | Sustained maximum velocity (cm/s) | 33.413 | 41.848 |
| 17 | Effective design acceleration (g) | 0.352 | 0.354 |
| 18 | A95 parameter (g) | 0.361 | 0.363 |
| 19 | Predominant period (s) | 0.220 | 0.180 |
| 20 | Significant duration (s) | 11.370 | 13.740 |

peak ground acceleration profile, excess pore pressure profile, and frequency content are collected.

3.2 Simplified Energy Concept

Jafarian et al. (2008, 2012, 2013) developed a new approach to determine liquefaction potential based on simplified kinetic energy density and originally based on the v_{max}/a_{max} ratio proposed by McGuire (1978). Jafarian et al. (2008) first formulated the simplified kinetic energy density as shown in Eq. (1).

$$MKED = \frac{1}{2}mv_{max,liq}^2 \tag{1}$$

where *MKED* is maximum kinetic energy density, *m* is soil mass, and $v_{max,liq}$ is maximum ground motion velocity to trigger liquefaction.

In Eq. 1, Jafarian et al. (2008) suggested the formulation of the v_{max}/a_{max} ratio for soil sites, from

McGuire (1978) as the main parameter in determining maximum kinetic energy density. However, Jafarian et al. (2008) mentioned that a more accurate evaluation of the v_{max}/a_{max} ratio may improve the performance of the model. Therefore, Jafarian et al. (2010) proposed new formulations to estimate the v_{max}/a_{max} as expressed in Eq. 2,

$$\frac{v_{max}}{a_{max}} = \left[\begin{array}{l} \ln(0.6348 \times 10^{-4}M_w^3(1.5211M_w - \ln V_{s30} + 0.0209R_{clstd}) \\ +0.5197) + 1.005) + N_S f_N(M_w) \\ + S_S f_S(M_w) + R_S f_R(M_w) \pm \sigma \end{array} \right] \tag{2a}$$

$$f_{(N)}(M_w) = 0.1647 \times 10^{-2}M_w(5.2019 - M_w) \tag{2b}$$

$$f_{(S)}(M_w) = -0.2805 \times 10^{-5}M_w^3(M - 0.9624) + 0.0318 \tag{2c}$$

$$f_{(R)}(M_w) = \left[\begin{array}{l} 0.3059 \times 10^{-4}M_w^3(0.0201M_w^2 - 0.0087M_w - 1) \\ (M_w - 1) \end{array} \right] \tag{2d}$$

where, M_w , R_{clstd} , V_{s30} , and σ are moment magnitude, closest distance from the site to the rupture area of fault (in km), time-averaged shear wave velocity for the first 30 m depth, and the total standard deviation of the equation ($\sigma=0.0643$), respectively. N_S , S_S , and R_S are the binary variables for normal, strike-slip, and reverse mechanisms, all of which have values between 0 and 1. Jafarian et al. (2010) also introduced fitting parameters related to earthquake magnitude; these are the normal (f_N), strike-slip (f_S), and reverse (f_R) mechanisms, respectively.

$$v_{max,liq} = \left[\begin{array}{l} \ln(0.6348 \times 10^{-4}M_w^3(1.5211M_w - \ln V_{s30}) \\ +0.0209R_{clstd} + 0.5197) + 1.005) + \\ N_S f_N(M_w) + S_S f_S(M_w) + R_S f_R(M_w) \pm \sigma \end{array} \right] a_{max} \times r_d \tag{3a}$$

$$\ln(r_d) = \left(0.01034 + 0.00321 \frac{PGA}{PGV} \right) z \tag{3b}$$

where r_d is the depth reduction factor, *z* is the analysed depth, *PGA* is the peak ground acceleration at the ground surface, and *PGV* is peak ground velocity at the ground surface.

MKED is a parameter that reflects the energy transfer experienced by soil layers during seismic wave propagation under the maximum motion parameters. Jafarian et al. (2008, 2010, 2012, 2013) stated that the

kinetic energy and *CSR* values modelled with the corrected SPT values or ($N_{1,60}$) have the same tendency in defining either zone of liquefaction or zone of no liquefaction. Therefore, this concept gives good results and benefits for the use of liquefaction potential based on seismic ground response in which the time-history components are considered. In line with the development of liquefaction prediction analysis, the prediction of liquefaction is possible to conduct using the energy concept. However, this concept is still rarely used to analyse the liquefaction potential. Hence, we set out in this study to demonstrate the implementation of seismic ground response analysis to obtain motion parameters used in kinetic energy density liquefaction assessment based on the conditions of Bengkulu City.

3.3 Analysis of Liquefaction Potential

On September 12, 2007, The M_w 8.6 earthquake hit Bengkulu City and its surrounding areas. Liquefaction was found in several areas, especially along Bengkulu’s coastal area. Mase (2018b) conducted reliability studies based on several empirical liquefaction methods, such as Seed et al. (1985); Tokimatsu and Yoshimi (1983); Japan Railway Association (1996); Youd and Idriss (2001); and Idriss and Boulanger (2006), Boulanger and Idriss (2014), to determine the liquefaction potentials of coastal areas in Bengkulu. Mase (2018b) also compared the predictions to field evidence and found that Idriss and Boulanger (2006) and the extended method, i.e., Boulanger and Idriss (2014) presented predictions that best-matched field evidence and thus was the most suitable method to predict liquefaction during an earthquake in Bengkulu City.

Boulanger and Idriss (2014) analysed liquefaction by determining the cyclic resistance ratio (*CRR*) from several intrinsic soil characteristics, and determining the cyclic stress ratio (*CSR*) from several external factors: *CRR* reflects the cyclic resistance provided by soils to counteract cyclical stress, while *CSR* reflects the cyclic stress which results from earthquake shaking. These two parameters were compared as an interpretation of liquefaction susceptibility reflected by a factor of safety or *FS*, as estimated by Eq. (4); *FS* less than 1 indicates that liquefaction may occur, whereas *FS* more or equal to 1 indicates that liquefaction may not occur.

$$FS = \frac{CRR}{CSR} \tag{4}$$

Generally, *CRR* is derived from site investigation data. In this study, the formula to determine *CRR* is derived CPT measurements based on the following equation,

$$CRR = \exp \left[\frac{q_{c1Ncs}}{113} + \left(\frac{q_{c1Ncs}}{1000} \right)^2 - \left(\frac{q_{c1Ncs}}{140} \right)^3 + \left(\frac{q_{c1Ncs}}{137} \right)^4 - 2.8 \right] \tag{5}$$

where, q_{c1Ncs} is a corrected cone resistance estimated by these equations (Idriss and Boulanger 2006)

$$q_{c1Ncs} = q_{c1N} + \Delta q_{c1N} \tag{6}$$

$$q_{c1N} = C_N(q_{cN}) \tag{7}$$

$$C_N = \left(\frac{P_a}{\sigma'_v} \right)^{1.338 - 0.249(q_{c1Ns})^{0.264}} \tag{8}$$

$$q_{cN} = \frac{q_c}{P_a} \tag{9}$$

$$\Delta q_{c1N} = \left(11.9 + \frac{q_{c1N}}{14.6} \right) \exp \left[1.63 - \frac{9.7}{FC + 2} - \left(\frac{15.7}{FC + 2} \right)^2 \right] \tag{10}$$

where, C_N is an overburden correction factor, q_c and q_{cN} are cone resistance and normalised cone resistances, P_a is atmospheric pressure (100 kPa), σ'_v is effective stress, *FC* is fines content, and Δq_{c1N} is the additional cone resistance depending on fines content.

Different from *CRR*, *CSR* depends on external factors that may trigger soil failure during earthquake shaking. Therefore, *CSR* is derived from the stresses resulting from earthquake shaking. *CSR* is determined based on the following equations,

$$CSR = 0.65 r_d \frac{PGA}{g} \frac{\sigma_v}{\sigma'_v} \frac{1}{MSF} \frac{1}{K_\sigma} \tag{11}$$

$$MSF = -0.058 + 6.9 \exp \left(-\frac{M_w}{4} \right) \leq 1.8 \tag{12}$$

$$K_\sigma = 1 - C_\sigma \ln \left(\frac{\sigma'_v}{P_a} \right) \leq 1.0 \tag{13}$$

$$C_\sigma = \frac{1}{37.3 - 8.27(q_{c1Ncs})^{0.264}} \leq 0.3 \quad (14)$$

where, r_d is a depth reduction factor estimated by Eq. (3b), σ'_v and σ_v are effective stress and total stress, MSF is a magnitude scaling factor estimated by Eq. (12) (Idriss 1999), M_w is moment magnitude, K_σ is an effective overburden pressure factor estimated by Eq. (13), C_σ is a factor for the overburden pressure factor, and P_a is atmospheric pressure (i.e., 100 kPa).

Post-liquefaction settlement estimation can be performed in analysis of ground response (Luo et al. 2019). According to Yoshimine et al. (2006) and Yi (2010), the prediction of post-liquefaction settlement can be estimated based on soil resistance and shaking impact. Firstly, the estimation of corrected shear wave velocity (V_{s1}) based on the model proposed by Idriss and Boulanger (2008) in Eq. 15,

$$V_{s1} = V_s \left(\frac{P_a}{\sigma'_v} \right)^{0.25} \quad (15)$$

Yi (2010) explained that the percentage of relative density (D_r) can be estimated using Eq. (16). V_{s1} is then corrected to the fines content to obtain the equivalent clean sand value or $(V_{s1})_{cs}$ (Andrus et al. 2004).

$$D_r = 17.94 \left[\frac{(V_{s1})_{cs}}{100} \right]^{1.976} \quad (16)$$

Ishihara and Yoshimine (1992) explained that there is relation between the volumetric strain (ϵ_v) of clean sand and shear strain (γ_{max}) and D_r during post-liquefaction reconsolidation. Yoshimine et al. (2006) suggested that ϵ_v can be estimated using Eq. 17,

$$\epsilon_v = 1.5 \exp(-2.5D_r) \cdot \min(0.08\gamma_{max}) \quad (17)$$

where D_r and γ_{max} are in decimal.

From Eqs. (15) to (17), the ground surface settlement for one-dimensional reconsolidation is then calculated by Eq. (18). The total settlement of post-liquefaction (S_{v-1D}) is calculated using the integration equation for volumetric strain and the depth interval of concern (Idriss and Boulanger 2008).

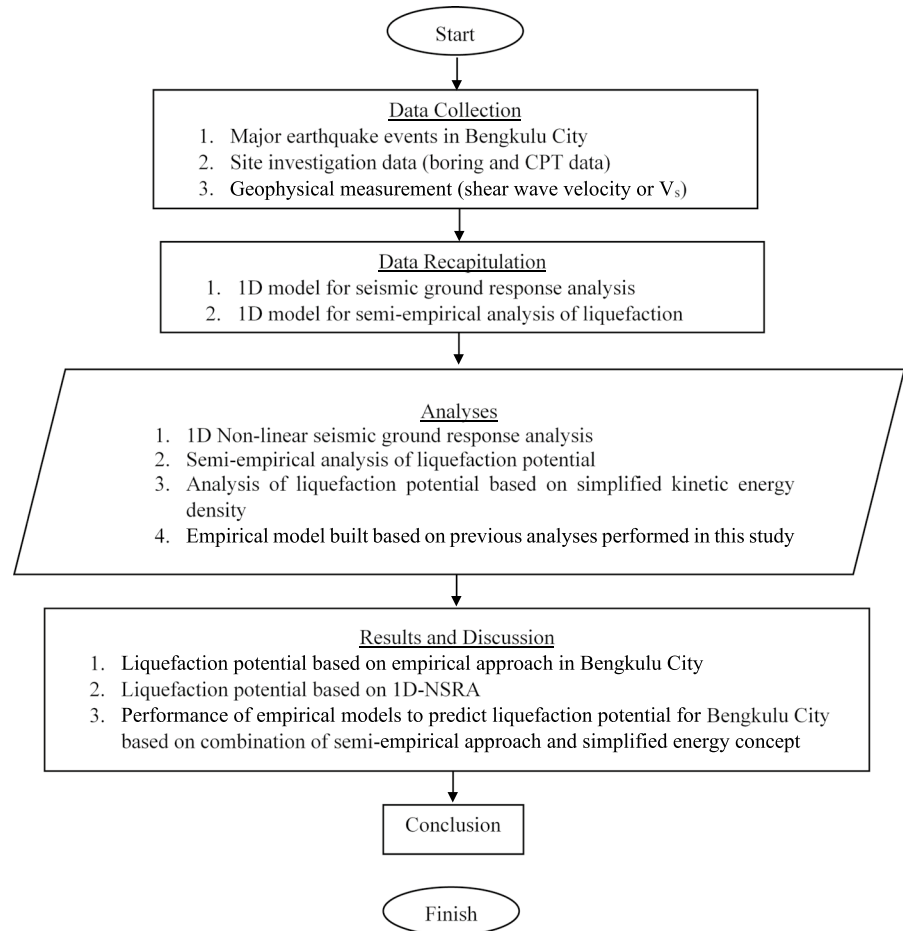
$$S_{v-1D} = \int_0^{z_{max}} \epsilon_v \cdot dz \quad (18)$$

3.4 Research Framework

Figure 6 shows the research framework implemented in this study. This study is initiated by capturing the issue of earthquakes in Bengkulu City, which is the area's primary form of natural disaster. A literature review into the earthquake backgrounds, geological conditions, liquefaction potential analysis procedures, kinetic energy concepts, and seismic ground response analyses could provide background for the rest of the study.

Data of past earthquake events in Bengkulu City were collected for use, including site investigation data (CPT results), and shear wave velocity (V_s) profiles (Fig. 4). The focus will be paid to the Bengkulu-Mentawai Earthquake in 2007 (M_w 8.6). Mase (2020) stated that the M_w 8.6 Bengkulu-Mentawai Earthquake was the most devastating in Bengkulu City; therefore, it is crucial to consider this earthquake for seismic hazard analysis.

Data recapitulation is then performed to assist in the analyses which follow. In this stage, a 1D model for NSRA and a 1D model for semi-empirical analysis of liquefaction potential are drawn. Afterward, the main analyses of this study are performed. First, 1D NSRA is performed by applying input motion (Fig. 5) at the bottom of investigated sites (i.e., at 30 m depth). Mase (2020), Misliniyati et al. (2018), and Mase (2017) suggested that the engineering bedrock surface in Bengkulu City is generally found at 30 m depth and is indicated by V_s values of 760 m/s. The use of $V_s = 760$ m/s to indicate the engineering bedrock surface was also suggested by several researchers such as Adampira et al. (2015), Mase et al. (2018), Misliniyati et al. (2019), and Likitlersuang et al. (2020). Therefore, this assumption is also implemented in this study. Several main results, such as acceleration profile, ground settlement, and so on are presented in this study. Semi-empirical analysis of liquefaction potential is performed based on PGA obtained from 1D NSRA. The acceleration profile from 1D NSRA is also used to estimate $MKED$, which is then correlated with the results of the semi-empirical analysis to generate empirical models of liquefaction predictions. Liquefaction potentials based on $MKED$, q_c , and FS are proposed and are presented. The performance of the proposed empirical models will be compared to previous studies to measure their reliability.

Fig. 6 Research framework

In general, the results of this study could provide a better understanding of liquefaction susceptibility in Bengkulu City. In addition, this study also proposes a new analysis framework to predict liquefaction. The proposed models will also be available for engineering practice in investigating liquefaction potential in Bengkulu City.

4 Results and Discussion

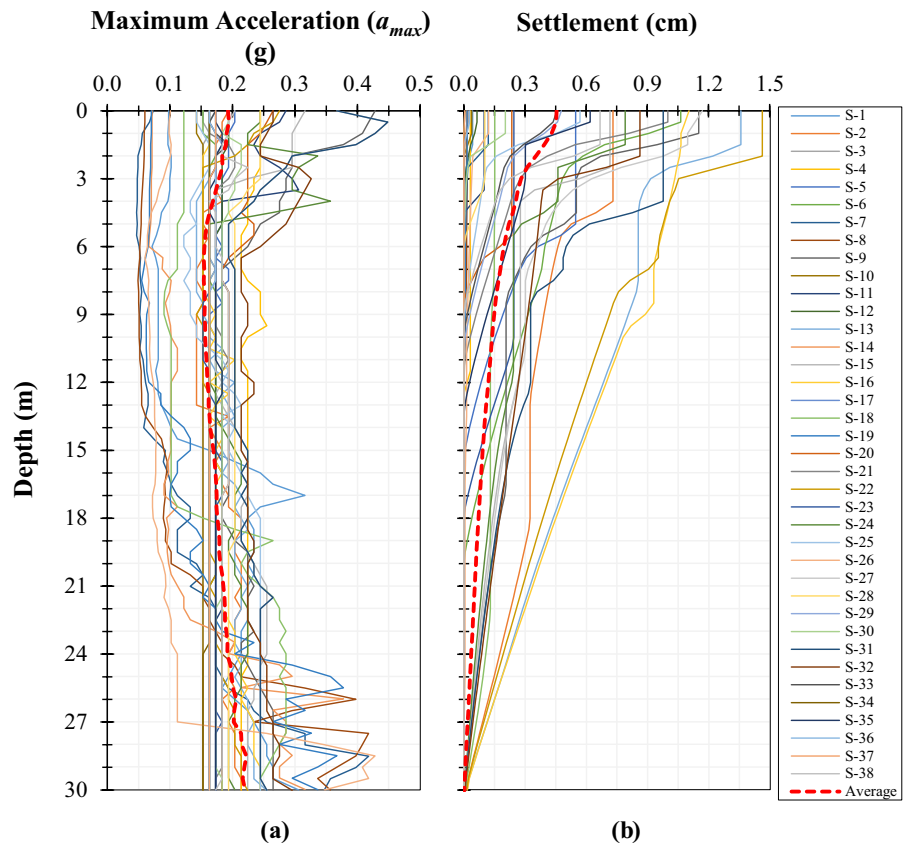
4.1 Ground Response and Settlement Prediction

Figure 7 presents the 1D-NSRA results which include the maximum acceleration (a_{max}) profile and ground settlement during the earthquake. Based on Fig. 7a, it can be seen that accelerations are relatively constant at 0.2 g from the bottom of investigated sites to the ground surface (dashed red line). Ground motions

slightly decrease as we move from 30 m depth to 15 m depth, then continuously increase up to the ground surface. As stated above, Kramer (1996) considers the triggering of liquefaction possible at a minimum PGA of 0.1 g. As such, the 1D NSRA does estimate that the investigated sites can undergo liquefaction, since their a_{max} values are, generally and on average, larger than 0.1 g. Several local studies performed by Misliniyati et al. (2018), Mase (2018a), and Mase (2020) mentioned that based on ground motion prediction using the model proposed by Idini et al. (2017), maximum acceleration during the Bengkulu-Mentawai Earthquake in 2007 was about 0.217 g, thus showing consistency between the results of this study and previous studies.

Ground settlement results from 1D NSRA are also presented in Fig. 7b. During a large earthquake, ground failure can be indicated by settlement observed at the ground surface. Based on the analysis,

Fig. 7 1D-NSRA results: **a** maximum acceleration profile, **b** ground settlement



the maximum settlement was about 1.5 cm. The average settlement due to the earthquake was about 0.5 cm. In general, the settlement results from 1D NSRA are consistent with field observations reported by Mase (2020) and Hausler and Anderson (2007), in which light to moderate settlement occurred along the coastal areas of Bengkulu City due to ground failure. Table 4 presents a recapitulation of PGA and maximum settlement data corresponding to the study area. In general, S-9 in Muara Bangkahulu District tended to have the maximum PGA in the study area (i.e., 0.428 g), while S-22 in Ratu Agung District had the maximum settlement of about 1.462 cm. Generally, the average PGA in Bengkulu City, which helps describe the area's most significant earthquake impact, is about 0.193 g.

4.2 Liquefaction Potential and Energy Density

The examples of liquefaction analysis result at representative sites are presented in Fig. 8. It should be noted that liquefaction only occurs in sand layers.

Therefore, in this study, clay layer FS values were set equal to zero. From Fig. 8, it can be seen that the entire analysed depth at S-23 has FS values less than 1, indicating potential liquefaction. Several sites, such as S-30 and S-37, have liquefaction potential at shallow depths. Liquefaction is also possible in some thick layers of S-7, S-26, and S-32. In addition, most of the liquefiable layers' ground acceleration (a_{max}) generally exceeded the liquefaction threshold of 0.1 g. In general, liquefaction in 2007 is observed the areas that were calculated as having high liquefaction potential as reported by Hausler and Anderson (2007) and Mase et al. (2020a, b). For example, the field evidence of liquefaction presented in Fig. 2 is located at S12, which was confirmed as a site with high liquefaction potential. Generally, liquefaction at the site is found at shallow depths from 0 to 1.5 m. Therefore, the sinking of the building in Fig. 2 occurred until 1.5 m depth below the ground surface.

Figure 9 presents the FS and MKED profiles at investigated sites. In Fig. 9a, FS against liquefaction is observed to vary from 0.197 to 5.986. In

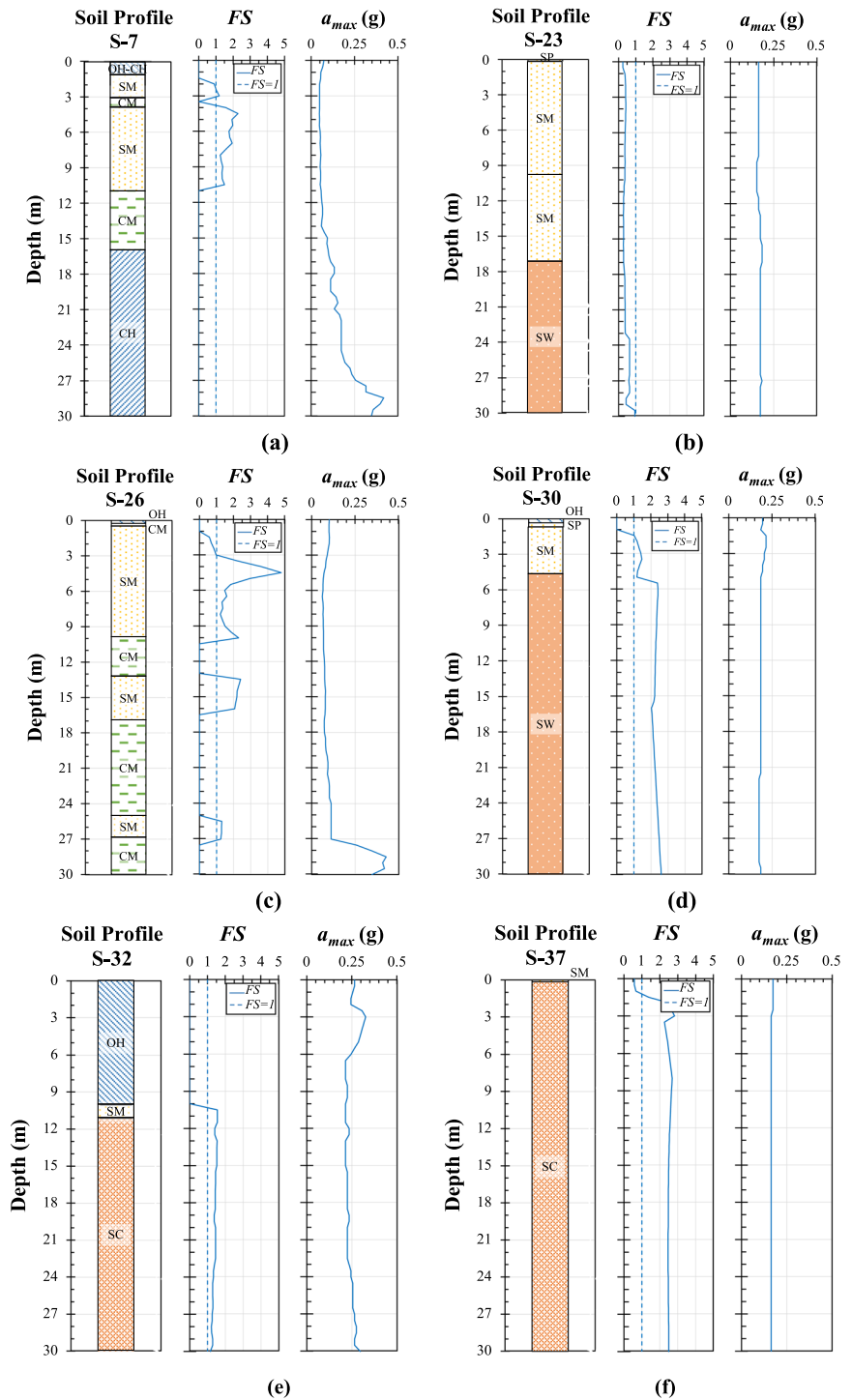
Table 4 Recapitulation of maximum acceleration and maximum settlement at ground surface

| No | Sites code | Location | | Districts | PGA (g) | Max settlement (cm) |
|----|------------|--------------|---------------|------------------|---------|---------------------|
| | | Latitude (°) | Longitude (°) | | | |
| 1 | S-1 | -3.758 | 102.259 | Muara Bangkahulu | 0.098 | 0.043 |
| 2 | S-2 | -3.743 | 102.252 | Muara Bangkahulu | 0.194 | 0.730 |
| 3 | S-3 | -3.780 | 102.262 | Muara Bangkahulu | 0.153 | 0.021 |
| 4 | S-4 | -3.759 | 102.277 | Muara Bangkahulu | 0.245 | 0.031 |
| 5 | S-5 | -3.766 | 102.271 | Muara Bangkahulu | 0.204 | 0.548 |
| 6 | S-6 | -3.753 | 102.271 | Muara Bangkahulu | 0.153 | 1.062 |
| 7 | S-7 | -3.778 | 102.283 | Muara Bangkahulu | 0.073 | 0.120 |
| 8 | S-8 | -3.751 | 102.292 | Muara Bangkahulu | 0.060 | 0.013 |
| 9 | S-9 | -3.768 | 102.291 | Muara Bangkahulu | 0.428 | 1.150 |
| 10 | S-10 | -3.784 | 102.260 | Teluk Segara | 0.143 | 0.038 |
| 11 | S-11 | -3.789 | 102.250 | Teluk Segara | 0.285 | 0.099 |
| 12 | S-12 | -3.798 | 102.253 | Teluk Segara | 0.194 | 0.064 |
| 13 | S-13 | -3.796 | 102.251 | Teluk Segara | 0.173 | 1.357 |
| 14 | S-14 | -3.798 | 102.255 | Teluk Segara | 0.071 | 0.014 |
| 15 | S-15 | -3.791 | 102.250 | Teluk Segara | 0.316 | 0.715 |
| 16 | S-16 | -3.809 | 102.265 | Ratu Samban | 0.163 | 1.103 |
| 17 | S-17 | -3.811 | 102.267 | Ratu Samban | 0.173 | 0.004 |
| 18 | S-18 | -3.816 | 102.273 | Ratu Samban | 0.122 | 0.151 |
| 19 | S-19 | -3.799 | 102.263 | Ratu Samban | 0.070 | 0.016 |
| 20 | S-20 | -3.818 | 102.276 | Ratu Agung | 0.265 | 0.235 |
| 21 | S-21 | -3.837 | 102.295 | Ratu Agung | 0.163 | 0.999 |
| 22 | S-22 | -3.852 | 102.305 | Ratu Agung | 0.275 | 1.462 |
| 23 | S-23 | -3.797 | 102.283 | Ratu Agung | 0.163 | 0.244 |
| 24 | S-24 | -3.818 | 102.285 | Ratu Agung | 0.245 | 0.791 |
| 25 | S-25 | -3.782 | 102.293 | Sungai Serut | 0.143 | 0.568 |
| 26 | S-26 | -3.790 | 102.326 | Sungai Serut | 0.101 | 0.120 |
| 27 | S-27 | -3.816 | 102.288 | Singaran Pati | 0.367 | 1.169 |
| 28 | S-28 | -3.821 | 102.309 | Gading Cempaka | 0.245 | 0.103 |
| 29 | S-29 | -3.868 | 102.319 | Selebar | 0.163 | 0.478 |
| 30 | S-30 | -3.850 | 102.350 | Selebar | 0.194 | 0.203 |
| 31 | S-31 | -3.837 | 102.322 | Selebar | 0.367 | 0.976 |
| 32 | S-32 | -3.880 | 102.353 | Selebar | 0.265 | 0.863 |
| 33 | S-33 | -3.890 | 102.322 | Kampung Melayu | 0.173 | 0.456 |
| 34 | S-34 | -3.915 | 102.308 | Kampung Melayu | 0.163 | 0.004 |
| 35 | S-35 | -3.930 | 102.287 | Kampung Melayu | 0.173 | 0.619 |
| 36 | S-36 | -3.938 | 102.284 | Kampung Melayu | 0.163 | 0.028 |
| 37 | S-37 | -3.938 | 102.289 | Kampung Melayu | 0.173 | 0.004 |
| 38 | S-38 | -3.930 | 102.304 | Kampung Melayu | 0.204 | 0.668 |

general, *FS* values less than one are found at shallow depths (Fig. 9a). Hausler and Anderson (2007) and Mase (2017) stated that liquefaction at a shallow depth can influence the performance of low-rise buildings. This is because the placement of low-rise

buildings is generally at a shallow depth. As such, it is necessary to design foundations for low-rise buildings that pay attention to the effects of liquefaction on the buildings. Farid and Mase (2020) and Mase et al. (2021a, b, c) also suggested that seismic

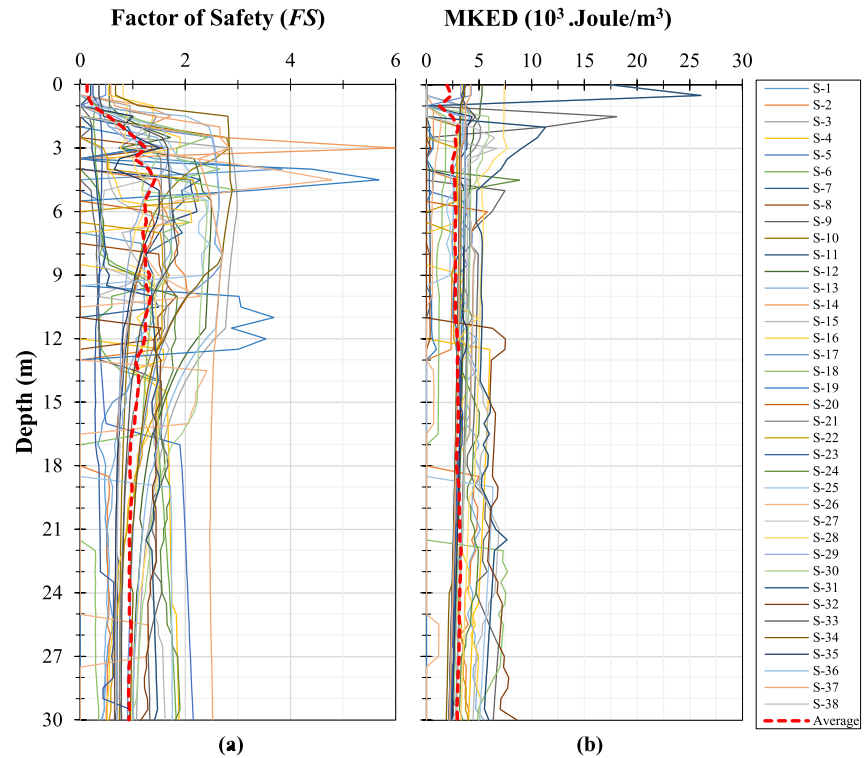
Fig. 8 Liquefaction potential at representative sites: **a** S-7, **b** S-23, **c** S-26, **d** S-30, **e** S-32, **f** S-37



hazard assessment should be considered for structure designs in Bengkulu City. When relating to geological conditions, the areas of Bengkulu City

that are prone to liquefaction are generally dominated by Q_{at} (Mase 2020). These areas correspond to several government building complexes, tourism

Fig. 9 Liquefaction potential: **a** profile of FS, **b** profile of MKED



locations, and business areas (Mase 2018a), all of which are certainly important areas of Bengkulu City whose susceptibility to seismic impacts should be considered.

Figure 9b presents the maximum kinetic energy density (*MKED*) of each investigated site. To calculate the amount of kinetic energy in the liquefied soil, it is necessary to first know a_{max} per each investigated depth. Thus, a_{max} was obtained from ground response analysis (Fig. 7a) and then used to estimate *MKED*. In Fig. 9b, the estimated values of *MKED* generally observed vary from 0.279 up to 26.056 kJ/m³. Based on Fig. 9b, sites with low *FS* values tend to have large *MKED* values. Thus, a larger *MKED* means a larger liquefaction potential (Jafarian et al. 2013). *MKED* value is also influenced by the magnitude of a_{max} . Larger *MKED* values correspond to larger a_{max} and vice versa. Earthquake waves that propagate on loose sandy soil layers tend to decrease soil stiffness (Yoshida 2015). In general cases, earthquake shaking could increase excess pore pressure and reduce the effective stress of sandy soil. This condition could lead to soil layers losing their strength and then becoming susceptible to liquefaction.

4.3 Empirical Models to Estimate Liquefaction Potential

The analysis results of this study were compiled into three charts that can be used to estimate liquefaction potential for Bengkulu City, shown in Figs. 10, 11 and 12. Mase (2020) recommended that the structural designs and soil resistance designs within earthquake-vulnerable areas should refer to a deterministic hazard analysis that considers the most significant earthquake. Therefore, these charts are in line with the recommendation since they refer to the Bengkulu-Mentawai Earthquake in 2007 and will be particularly useful for Bengkulu City and its vicinity area. These charts illustrate the correlations between three important parameters: *FS*, q_{cIN} , and *MKED*; *FS* represents the level of liquefaction susceptibility, q_{cIN} represents the availability of soil resistance (internal factor), and *MKED* represents the external factor that can trigger liquefaction. The models have been proposed in the terminology of the median, upper boundaries, and lower boundaries, which when combined provide information that minimises uncertainty. The proposed models are also validated by comparison to previous

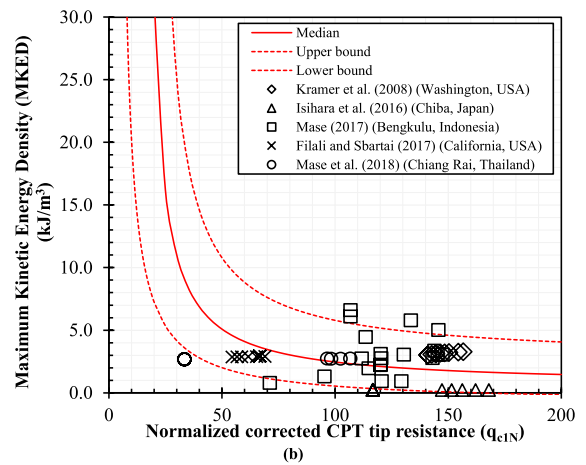
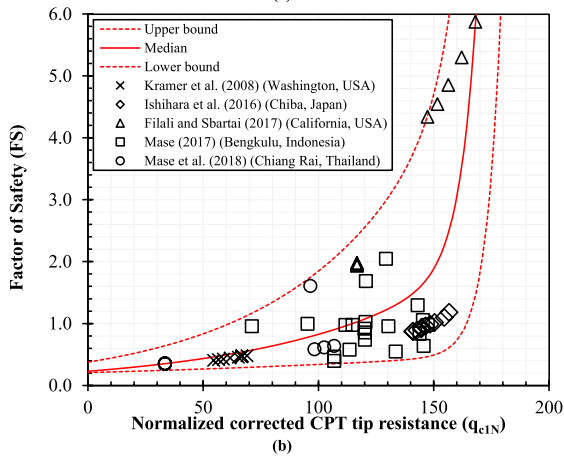
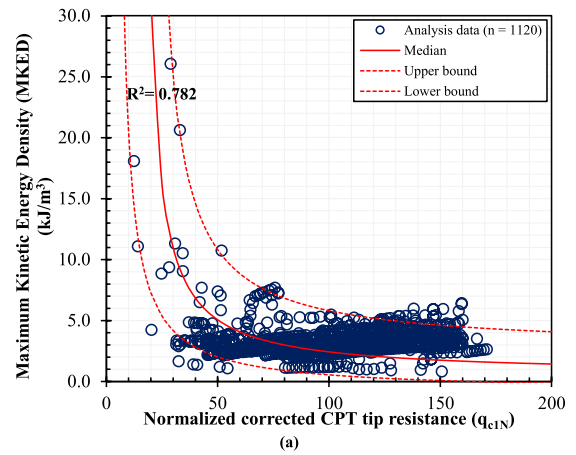
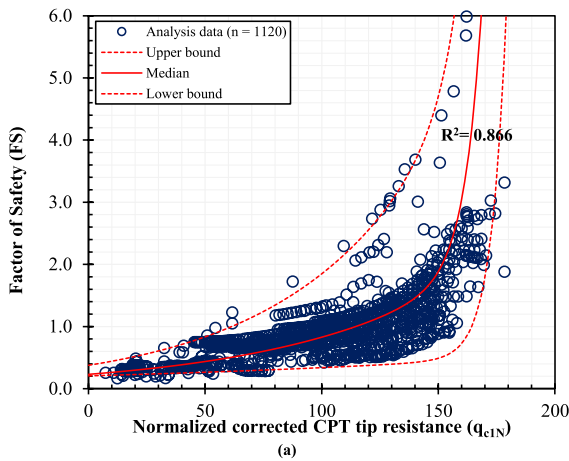


Fig. 10 Proposed charts to estimate FS from q_{c1N} **a** the development of chart for FS estimation from q_{c1N} **b** the performance of chart to worldwide cases

Fig. 11 Proposed charts to estimate MKED from q_{c1N} **a** the development of chart for MKED estimation from q_{c1N} **b** the performance of chart to worldwide cases

studies conducted in various regions having site characteristics dominated by sandy soils. to observe the consistency of the models. Previous studies used for comparison include Kramer (2008) conducted in Washington, USA; Ishihara et al. (2016) in Chiba, Japan; Filali and Sbartaï (2017) in California, USA; Mase (2017) in Bengkulu, Indonesia; and Mase et al. (2018) in Chiang Rai, Thailand.

Figures 10, 11 and 12 show the correlations for empirical prediction of liquefaction potential. In general, correlations presented in Figs. 10, 11 and 12 are derived based on data distribution. The regression analysis is conducted on the data distribution for MKED, FS, and q_{c1N} . From the data distribution, the empirical predictions for MKED, FS, and q_{c1N} are proposed in Eqs. 15 to 17. For trendlines, the proposed

charts had coefficients of determination (R^2) of more than 0.75. It indicates that all parameters had a strong correlation with each other. However, based on data distribution, it is also shown in Figs. 10, 11 and 12, there are uncertainties found in the results. Therefore, the upper and lower boundaries are proposed.

Figure 10 presents the plot to determine FS from q_{c1N} . It can be seen that FS increases with q_{c1N} . The upper boundary, median, and lower boundary of the correlation between q_{c1N} and FS are described by Eqs. (19). At the crucial value of $FS=1$, the values of q_{c1N} are observed to vary between 50 and 170. Many sites in Bengkulu City are composed of sand and fine material mixtures, which (loose sands) according to Kusumawardani et al. (2016) and Mase et al. (2019) are sensitive to liquefaction during cyclic loading.

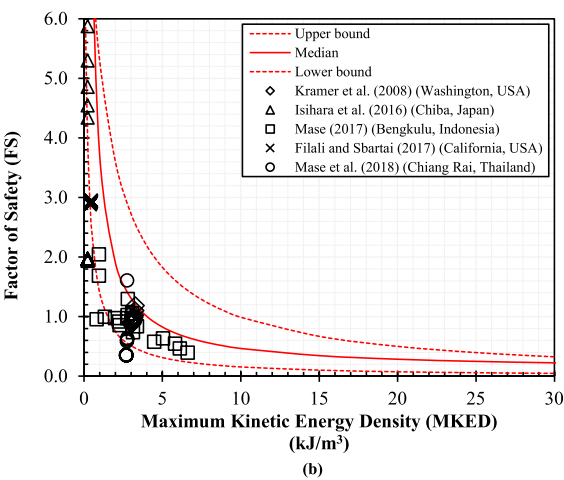
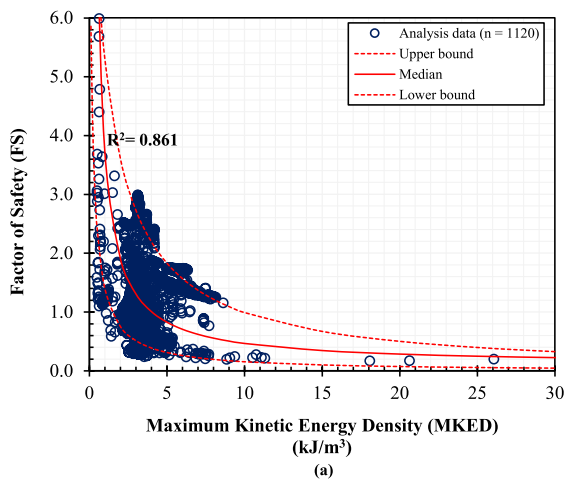


Fig. 12 Proposed charts to estimate FS from MKED **a** the development of chart for FS estimation from MKED **b** the performance of chart to worldwide cases

Site investigations revealed that sand layers with q_{c1N} less than 50, were generally found at shallow depths. It is therefore logical to deduce that liquefaction may commonly occur at shallow depths in Bengkulu City.

$$FS_{UB} = 0.3766 \times \exp(0.0159q_{c1N}) + 4.259 \cdot 10^{-9} \times \exp(0.1253q_{c1N}) \tag{19a}$$

$$FS_{mean} = (2.9834 \times 10^{-10}) \times \exp(0.1386q_{c1N}) + 0.23 \times \exp(0.0128q_{c1N}) \tag{19b}$$

$$FS_{LB} = (3.152 \times 10^{-12}) \times \exp(0.1575q_{c1N}) + 0.208 \times \exp(0.0049q_{c1N}) \tag{19c}$$

Figure 11 presents the plot to estimate $MKED$ from q_{c1N} . Since $MKED$ is derived from a_{max} , an estimation of $MKED$ is analogous to estimating the required a_{max} to trigger liquefaction. Based on Fig. 11, $MKED$ increases substantially at q_{c1N} less than 50, with the highest $MKED$ from our analysis reaching about 26 kJ/m³. At the critical condition of $FS = 1$, the $MKED$ is about 2 kJ/m³ (directly observable in Fig. 12, discussed below). The upper boundary, median, and lower boundary of this relationship are described by Eqs. (20),

$$MKED_{UB} = \frac{76.3391 + q_{c1N}}{-6.989 + 0.3735q_{c1N}} \tag{20a}$$

$$MKED_{mean} = \frac{247.2786 + q_{c1N}}{-24.958 + 1.6715q_{c1N}} \tag{20b}$$

$$MKED_{LB} = \frac{-160.937 + q_{c1N}}{4.5682 + 1.2010q_{c1N}} \tag{20c}$$

Figure 12 presents the correlation between FS and $MKED$, with the upper boundary, median, and lower boundary described by Eqs. (21). As previously elaborated, liquefaction occurs at $FS < 1$, which corresponds to $MKED > 2$ kJ/m³.

$$FS_{UB} = -0.0439 + \left(\frac{11.5411}{1.1620 + MKED} \right) \tag{21a}$$

$$FS_{mean} = 0.1072 + \frac{3.6907}{0.0014 + MKED} \tag{21b}$$

$$FS_{LB} = 0.0078 + \frac{1.6627}{0.1837 + MKED} \tag{21c}$$

We understand that the use of the proposed equations is relevant for liquefaction potential in Bengkulu City. In this study, the comparison

to liquefaction cases in other areas is to confirm whether the models are relevant for general implementation or not. Based on the comparison, some worldwide cases can be relevant to the chart we proposed. When we plotted the data from studies conducted in Washington, USA (Kramer 2008); Chiba, Japan (Ishihara et al. 2016); Bengkulu, Indonesia (Mase 2017); California, USA (Filali and Sbartai 2017); and Chiang Rai, Thailand (Mase et al. 2018; Mase and Likitlersuang 2021) against the boundaries and median of Fig. 12, we found that almost all of these studies' data points fall within the proposed range. This gives us reasonable confidence that the proposed charts could accurately predict liquefaction potential in Bengkulu City. In addition, although these plots and equations describing the relationships between FS , q_{cIN} and $MKED$ were derived based on data from Bengkulu City, it seems that they may be appropriate for describing worldwide cases as well.

5 Conclusion

A simplified energy concept for liquefaction prediction was applied for Bengkulu City. A total of 38 sites in the city were studied. The empirical analysis results were correlated to generate empirical equations that can predict liquefaction potential in the study area. Several concluding remarks can be drawn:

1. In past earthquake events, liquefactions in Bengkulu City were mostly found at shallow depths which implies that liquefaction could influence the performance of low-rise building structures during large earthquakes.
2. Loose to medium sandy soil layers in the study area are vulnerable to liquefaction. Those are found in areas with alluvium terraces (Qat) geological formations. One of the developed correlations will allow for the identification of areas susceptible to liquefaction through cone penetration tests. More specifically, areas identified with $q_{cIN} > 50$ will, according to the correlation, be at the critical value of factor of safety against liquefaction ($FS = 1$) and be susceptible to liquefaction. The amount of energy value ($MKED$) that propagates in each layer of soil depends on the value PGA . It is estimated that liquefaction may occur at $MKED > 2 \text{ kJ/m}^3$.
3. The simplified energy concept correlations developed in this study also relatively accurately described data obtained during previous studies from various sites around the world. As such, the framework implemented in this study could potentially be adopted to estimate the liquefaction potential of other areas outside of Bengkulu City.

Acknowledgements The authors would like to acknowledge the Research and Community Services Agency, University of Bengkulu, for funding collaborative research 2020 (with Ref. No. 2058/UN30.15/LT/2020) under the scheme of International Collaboration Research. This study was also partially supported by the World Class Professor 2021 (with Ref. No. 2817/E4.1/KK.04.05/2021) Program from the Ministry of Education, Culture, Research and Technology, Republic of Indonesia. The sixth author (W. Tanapalungkorn) acknowledges the C2F Fund for Postdoctoral Fellowship, Chulalongkorn University, Thailand. The last author (S. Likitlersuang) acknowledges the funding from the National Research Council of Thailand (NRCT). The authors would also like to thank all people who have contributed to this research.

Funding It is not applicable in this case.

Data Availability All the datasets that have been used and analysed during the current study are available from the corresponding author upon reasonable request.

Declarations

Conflict of interest The Authors declare that there are no competing interests.

References

- Adampira M, Alielahi H, Panji M, Koohsari H (2015) Comparison of equivalent linear and nonlinear methods in seismic analysis of liquefiable site response due to near-fault incident waves: a case study. *Arab J Geosci* 8(5):3103–3118. <https://doi.org/10.1007/s12517-014-1399-6>
- Amini PF, Noorzad R (2018) Energy-based evaluation of liquefaction of fiber-reinforced sand using cyclic triaxial testing. *Soil Dyn Earthq Eng* 104:45–53. <https://doi.org/10.1016/j.soildyn.2017.09.026>
- Andrus RD, Stokoe KH, Hsein Juang C (2004) Guide for shear-wave-based liquefaction potential evaluation. *Earthq Spectra* 20(2):285–308. <https://doi.org/10.1193/1.171510>
- Azeiteiro RJ, Coelho PA, Taborda DM, Grazina JC (2017) Energy-based evaluation of liquefaction potential under non-uniform cyclic loading. *Soil Dyn Earthq Eng*

- 92:650–665. <https://doi.org/10.1016/j.soildyn.2016.11.005>
- Berrill JB, Davis RO (1985) Energy dissipation and seismic liquefaction of sands: revised model. *Soils Found* 25(2):106–118. https://doi.org/10.3208/sandf1972.25.2_106
- Boulanger RW, Idriss IM (2014) CPT and SPT based liquefaction triggering procedures. Report No. UCD/CGM-14/01, Centre for Geotechnical Modeling, Dept of Civil Engineering, University of California at Davis, California (state), 138 pp. http://www.ce.memphis.edu/7137/PDFs/Notes/i3Boulanger_Idriss_CPT_and_SPT_Liq_triggering_CGM-14-01_20141.pdf
- Bowden DC, Tsai VC (2017) Earthquake ground motion amplification for surface waves. *Geophys Res Lett* 44(1):121–127. <https://doi.org/10.1002/2016GL071885>
- de Magistris FS, Lanzano G, Forte G, Fabbrocino G (2013) A database for PGA threshold in liquefaction occurrence. *Soil Dyn Earthq Eng* 54:17–19. <https://doi.org/10.1016/j.soildyn.2013.07.011>
- Dong L, Luo Q (2022) Investigations and new insights on earthquake mechanics from fault slip experiments. *Earth Sci Rev* 228(104019):1–17. <https://doi.org/10.1016/j.earscirev.2022.104019>
- Elgamal A, Yang Z, Lu J (2006) “Cyclic1D: A Computer Program for Seismic Ground Response”. Report No. SSRP-06/05, Department of Structural Engineering, University of California, San Diego, California (state), 28pp. http://soilquake.net/cyclic1d/Cyclic1D_UserManual.pdf
- Farid M, Mase LZ (2020) Implementation of seismic hazard mitigation on the basis of ground shear strain indicator for spatial plan of Bengkulu City, Indonesia. *Int J Geomate* 18(69):199–207. <https://doi.org/10.21660/2020.69.24759>
- Figueroa JL, Saada AS, Liang L, Dahisaria NM (1994) Evaluation of soil liquefaction by energy principles. *J Geotech Eng* 120(9):1554–1569. [https://doi.org/10.1061/\(ASCE\)07339410\(1994\)120:9\(1554\)](https://doi.org/10.1061/(ASCE)07339410(1994)120:9(1554))
- Filali K, Sbartaï B (2017) A comparative study between simplified and nonlinear dynamic methods for estimating liquefaction potential. *J Rock Mech Geotech Eng* 9(5):955–966. <https://doi.org/10.1016/j.jrmge.2017.05.008>
- Green RA, Mitchell JK (2004) Energy-based evaluation and remediation of liquefiable soils. In: Yegian MK, Kavazanjian E (eds) *Geotechnical Engineering for Transportation Projects*. ISBN: 9780784407448, American Society of Civil Engineers (ASCE), USA, pp 1961–1970.
- Hancock J, Watson-Lamprey J, Abrahamson NA, Bommer JJ, Markatis A, McCoy EMMA, Mendis R (2006) An improved method of matching response spectra of recorded earthquake ground motion using wavelets. *J Earthquake Eng* 10(1):67–89. <https://doi.org/10.1080/13632460609350629>
- Hausler E, Anderson A (2007) Observation of the 12 and 13 September 2007 Earthquake, Sumatra, Indonesia. Build Change Report, Colorado, 15pp. https://buildchange-web.s3.amazonaws.com/resources/tech/BC_Bengkulu_English.pdf
- Idini B, Rojas F, Ruiz S, Pastén C (2017) Ground motion prediction equations for the Chilean subduction zone. *Bull Earthq Eng* 15(5):1853–1880. <https://doi.org/10.1007/s10518-016-0050-1>
- Idriss IM, Boulanger RW (2008) Soil liquefaction during earthquakes. Earthquake Engineering Research Institute.
- Idriss IM, Boulanger RW (2006) Semi-empirical procedures for evaluating liquefaction potential during earthquakes. *Soil Dyn Earthq Eng* 26(2–4):115–130. <https://doi.org/10.1016/j.soildyn.2004.11.023>
- Idriss IM (1999) An update to the Seed-Idriss simplified procedure for evaluating liquefaction potential. In: Proceeding of TRB Workshop on New Approaches to Liquefaction, 10 January 1999, Washington, USA.
- Ishihara K, Harada K, Lee WF, Chan CC, Safiullah AMM (2016) Post-liquefaction settlement analyses based on the volume change characteristics of undisturbed and reconstituted samples. *Soils and Foundations* 56(3):533–546. <https://doi.org/10.1016/j.sandf.2016.04.019>
- Ishihara K, Yoshimine M (1992) Evaluation of settlements in sand deposits following liquefaction during earthquakes. *Soils Found* 32(1):173–188. <https://doi.org/10.3208/sandf1972.32.173>
- Jafarian Y, Kermani E, Baziar MH (2010) Empirical predictive model for the v_{max}/a_{max} ratio of strong ground motions using genetic programming. *Comput Geosci* 36(12):1523–1531. <https://doi.org/10.1016/j.cageo.2010.07.002>
- Jafarian YANT, Towhata I, Baziar MH, Noorzad A, Bahmanpour A (2012) Strain energy-based evaluation of liquefaction and residual pore water pressure in sands using cyclic torsional shear experiments. *Soil Dyn Earthq Eng* 35:13–28. <https://doi.org/10.1016/j.soildyn.2011.11.006>
- Jafarian Y, Vakili R, Abdollahi AS (2013) Prediction of cyclic resistance ratio for silty sands and its applications in the simplified liquefaction analysis. *Comput Geotech* 52:54–62. <https://doi.org/10.1016/j.compgeo.2013.04.001>
- Jafarian Y, Vakili R, Sadhegi AR, Sharafi H and Baziar MH (2008) A New Simplified Criterion for The Assessment of Field Liquefaction Potential Based on Dissipated Kinetic Energy. In: The 14th World Conference of Earthquake Engineering, 12–17 October 2008, Beijing, China.
- JRA (Japan Rail Association) (1996) Design code and explanation for roadway bridges-seismic resistance design 1995 revision. Japan Rail Association, Japan
- Kayen RE, Mitchell JK (1997) Assessment of liquefaction potential during earthquakes by Arias intensity. *J Geotech Geoenviron Eng ASCE* 123(12):1162–1174. [https://doi.org/10.1061/\(ASCE\)1090-0241\(1997\)123:12\(1162\)](https://doi.org/10.1061/(ASCE)1090-0241(1997)123:12(1162))
- Kokusho T (2013) Liquefaction potential evaluations: energy-based method versus stress-based method. *Can Geotech J* 50(10):1088–1099. <https://doi.org/10.1139/cgj-2012-0456>
- Kramer SL (1996) *Geotechnical earthquake engineering*. ISBN-13: 978-0133749434. Pearson Education, India, 672pp.
- Kramer SL (2008) Evaluation of liquefaction hazards in Washington state. Report No. WA-RD 668.1, Dept. of Transportation, Office of Research and Library Services, Washington (State), 329pp. <https://www.wsdot.wa.gov/research/reports/fullreports/668.1.pdf>
- Kundu A, Patra NR, Bandyopadhyay S, Reddy GR (2021) Static and dynamic characterization and response analysis of soils from Northern India. *SN Appl Sci* 3(2):1–15. <https://doi.org/10.1007/s42452-021-04196-1>
- Kusumawardani R, Suryolelono KB, Suhendro B, Rifa'i A (2016) The dynamic response of unsaturated clean sand at

- a very low frequency. *Int J Technol* 7(1): 123–131. <https://doi.org/10.14716/ijtech.v7i1.1163>
- Kusumawardani R, Chang M, Upomo TC, Huang RC, Fansuri MH, Prayitno GA (2021) Understanding of Petobo liquefaction flowslide by 2018.09. 28 Palu-Donggala Indonesia earthquake based on site reconnaissance. *Landslides* 18(9):3163–3182. <https://doi.org/10.1007/s10346-021-01700-x>
- Li B, Pandey MD, Dai KS, Lu Y, Zhou YZ, Shi YF, Ding ZB (2019) Effects of soil parameter variabilities on the estimation of ground-motion amplification factors. *Earthq Spectra* 35(2):907–928. <https://doi.org/10.1193/053118EQS131M>
- Likitlersuang S, Plengsiri P, Mase LZ, Tanapalungkorn W (2020) Influence of spatial variability of ground on seismic response analysis: a case study of Bangkok subsoils. *Bull Eng Geol Env* 79(1):39–51. <https://doi.org/10.1007/s10064-019-01560-9>
- National Research Council (1985) Liquefaction of soils during earthquakes, Committee on Earthquake Engineering, National Research Council (U.S.), 1985.
- Luo L, Lu J, Elgarni A, Fraser M (2019) Estimation of liquefaction induced settlement from computed seismic site response. In: Silvestri F, Moraci N (eds) *Earthquake geotechnical engineering for protection and development of environment and constructions*. CRC Press, Florida, pp 3692–3699
- Mase LZ (2018b) The reliability study of empirical analysis method of liquefaction potential due to the M_w 8.6 September 12, 2007 Earthquake in Coastal Area of Bengkulu City. *Civil Eng J* 25(1):53–60. [https://doi.org/10.5614/jts.2018.25.1.7\(InIndonesian\)](https://doi.org/10.5614/jts.2018.25.1.7(InIndonesian))
- Mase LZ (2020) Seismic hazard vulnerability of Bengkulu City, Indonesia, based on deterministic seismic hazard analysis. *Geotech Geol Eng* 38(4):5433–5455. <https://doi.org/10.1007/s10706-020-01375-6>
- Mase LZ (2021) A note of ground motion interpretation and site response analysis during the 2007 Bengkulu-Mentawai earthquakes, Indonesia. *Arab J Geosci* 14(2):1–14
- Mase LZ (2022) Local seismic hazard map based on the response spectra of stiff and very dense soils in Bengkulu city, Indonesia *Geodesy Geodyn* 13(6):573–584. <https://doi.org/10.1016/j.geog.2022.05.003>
- Mase LZ, Likitlersuang S, Tobita T (2018) Non-linear site response analysis of soil sites in Northern Thailand during the M_w 6.8 Tarlay earthquake. *Eng J* 22(3):291–303. <https://doi.org/10.4186/ej.2018.22.3.291>
- Mase LZ, Likitlersuang S, Tobita T (2019) Cyclic behaviour and liquefaction resistance of Izumio sands in Osaka, Japan. *Mar Georesour Geotechnol* 37(7):765–774. <https://doi.org/10.1080/1064119X.2018.1485793>
- Mase LZ, Likitlersuang S, Tobita T, Chitrakaikeow S, Sorlump S (2020a) Local site investigation of liquefied soils caused by earthquake in Northern Thailand. *J Earthquake Eng* 24(7):1181–1204. <https://doi.org/10.1080/13632469.2018.1469441>
- Mase LZ, Refrizon R, Anggraini PW (2021a) Local site investigation and ground response analysis on downstream area of Muara Bangkahulu River, Bengkulu City, Indonesia. *Indian Geotech J* 51(5):952–966. <https://doi.org/10.1007/s40098-020-00480-w>
- Mase LZ, Sugianto N, Refrizon (2021b) Seismic hazard microzonation of Bengkulu City, Indonesia. *Geoenviron Disasters* 8(5):1–17. <https://doi.org/10.1186/s40677-021-00178-y>
- Mase LZ, Likitlersuang S, Tobita T (2022a) Verification of liquefaction potential during the strong earthquake at the border of Thailand-Myanmar. *J Earthquake Eng* 26(4):2023–2050. <https://doi.org/10.1080/13632469.2020.1751346>
- Mase LZ, Likitlersuang S (2021) Implementation of seismic ground response analysis to estimate liquefaction potential in Northern Thailand. *Indonesian J Geosci* 8(3): 371–383. <https://doi.org/10.17014/ijog.8.3.329-341>
- Mase LZ, Somantri AK (2016) Development of Spectral Response Design for Bengkulu City Based on Deterministic Approach. In: *Proceedings of the 20th Annual Meeting of Indonesian Society for Geotechnical Engineering*, 15–16 November, Jakarta, Indonesia.
- Mase LZ, Farid M, Sugianto N, Agustina S (2020b) The Implementation of ground response analysis to quantify Liquefaction Potential Index (LPI) in Bengkulu City, Indonesia. *J Civil Eng Forum* 6(3):319–330. <https://doi.org/10.22146/jcef.57466>
- Mase LZ, Fathani TF, Adi AD (2021a) A Simple Shaking Table Test to Measure Liquefaction Potential of Prambanan Area, Yogyakarta, Indonesia. *ASEAN Eng J* 11(3):89–108. <https://doi.org/10.11113/aej.v11.16874>
- Mase LZ, Tanapalungkorn W, Likitlersuang S, Ueda K, Tobita T (2022b) Liquefaction analysis of Izumio sands under variation of ground motions during strong earthquake in Osaka, Japan. *Soils Foundations* 62(5):101218. <https://doi.org/10.1016/j.sandf.2022.101218>
- Mase LZ (2017) Liquefaction potential analysis along coastal area of Bengkulu Province due to the 2007 M_w 8.6 Bengkulu earthquake. *J Eng Technol Sci* 49(6):721–736. <https://doi.org/10.5614/j.eng.technol.sci.2017.49.6.2>
- Mase LZ (2018a) Reliability study of spectral acceleration designs against earthquakes in Bengkulu City, Indonesia. *Int J Technol* 9(5):910–924. <https://doi.org/10.14716/ijtech.v9i5.621>
- McCaffrey R (2009) The tectonic framework of the Sumatran subduction zone. *Annu Rev Earth Planet Sci* 37(1):345–366. <https://doi.org/10.1146/annurev.earth.031208.100212>
- McGuire RK (1978) Seismic ground motion parameter relations. *J Geotech Eng Divis ASCE* 104(4):481–490. <https://doi.org/10.1061/AJGEB6.0000615>
- Misliniyati R, Mase LZ, Syahbana AJ and Soebowo, E (2018) Seismic hazard mitigation for Bengkulu Coastal area based on site class analysis. *IOP Conf Ser Earth Environ Sci* 212(1):012004. <https://doi.org/10.1088/1755-1315/212/1/012004>
- Misliniyati R, Mase LZ, Irsyam M, Hendriawan, Sahadewa A (2019) Seismic response validation of simulated soil models to vertical array record during a strong earthquake. *J Eng Technol Sci* 51(6):772–790. <https://doi.org/10.5614/j.eng.technol.sci.2019.51.6.3>
- Naik SP, Kundu A, Patra NR, Bandopadhyaya S, Reddy GR (2022) Earthquake response analysis of soils from Rudrapur and Khatima Sites Adjacent to Himalayan Frontal Thrust (HFT) using field and laboratory-derived

- dynamic soil properties. *J Earthquake Eng* 26(2):949–979. <https://doi.org/10.1080/13632469.2019.1695691>
- Natawidjaja DH, Triyoso W (2007) The Sumatran fault zone—from source to hazard. *J Earthquake Tsunami* 1(1):21–47. <https://doi.org/10.1142/S1793431107000031>
- National Earthquake Hazards Reduction Program (NEHRP) (1998) Recommended provisions for seismic regulation for new building and other structure, 1997 edition, Part 1—provisions, Part 2—commentary. FEMA 302–303, Building Seismic Safety Council, Washington DC, 702pp.
- Natural Disaster Agency or BPBD Bengkulu Province (2018) Geological Map of Bengkulu City. Natural Disaster Agency or BPBD Bengkulu Province, Bengkulu, Indonesia, 1p.
- Nemat-Nasser S, Shokoh A (1979) A unified approach to densification and liquefaction of cohesionless sand in cyclic shearing. *Can Geotech J* 16(4):659–678. <https://doi.org/10.1139/t79-076>
- Rashidian V, Baise LG (2020) Regional efficacy of a global geospatial liquefaction model. *Eng Geo* 272:105644. <https://doi.org/10.1016/j.enggeo.2020.105644>
- Rezania M, Javadi AA, Giustolisi O (2010) Evaluation of liquefaction potential based on CPT results using evolutionary polynomial regression. *Comput Geotech* 37(1–2):82–92. <https://doi.org/10.1016/j.compege.2009.07.006>
- Robertson PK (2015) Comparing CPT and V s liquefaction triggering methods. *J Geotechn Geoenviron Eng* 141(9):04015037. [https://doi.org/10.1061/\(ASCE\)GT.1943-5606.0001338](https://doi.org/10.1061/(ASCE)GT.1943-5606.0001338)
- Robertson PK, Wride CE (1998) Evaluating cyclic liquefaction potential using the cone penetration test. *Can Geotech J* 35(3):442–459. <https://doi.org/10.1139/t98-017>
- Sana H, Nath SK (2016) Liquefaction potential analysis of the Kashmir valley alluvium, NW Himalaya. *Soil Dyn Earthq Eng* 85:11–18. <https://doi.org/10.1016/j.soildyn.2016.03.009>
- Seed HB, Tokimatsu K, Harder LF, Chung RM (1985) Influence of SPT procedures in soil liquefaction resistance evaluation. *J Geotechn Eng Div ASCE* 111(12):1425–1445. [https://doi.org/10.1061/\(ASCE\)0733-9410\(1985\)111:12\(1425\)](https://doi.org/10.1061/(ASCE)0733-9410(1985)111:12(1425))
- Sonmezer YB (2019) Energy-based evaluation of liquefaction potential of uniform sands. *Geomech Eng* 17(2):145–156. <https://doi.org/10.12989/gae.2019.17.2.145>
- Sukkarak R, Tanapalungkorn W, Likitlersuang S, Ueda K (2021) Liquefaction analysis of sandy soil during strong earthquake in Northern Thailand. *Soils Found* 61(5):1302–1318. <https://doi.org/10.1016/j.sandf.2021.07.003>
- Tokimatsu K, Yoshimi Y (1983) Empirical correlation of soil liquefaction based on SPT values and fines content. *Soils Found* 23(4):56–74. https://doi.org/10.3208/sandf1972.23.4_56
- Widiwijayanti C, Déverchère J, Louat R, Sébrier M, Harjono H, Diament M, Hidayat D (1996) Aftershock sequence of the 1994, Mw 6.8, Liwa earthquake (Indonesia): seismic rupture process in a volcanic arc. *Geophys Res Lett* 23(21):3051–3054. <https://doi.org/10.1029/96GL02048>
- Wiseman K, Banerjee P, Bürgmann R, Sieh K, Dreger DS, Hermawan I (2012) Source model of the 2009 Mw 7.6 Padang intraslab earthquake and its effect on the Sunda megathrust. *Geophys J Int* 190(3):1710–1722. <https://doi.org/10.1111/j.1365-246X.2012.05600.x>
- Yi F (2010) Procedure to evaluate liquefaction-induced lateral spreading based on shear wave velocity. In: Proceedings of international conferences on recent advances in geotechnical earthquake engineering and soil dynamics, 24–29 May, CA, USA.
- Yılmaz D, Babuçcu F, Batmaz S, Kavruk F (2008) Liquefaction analysis and soil improvement in Beydag dam. *Geotech Geol Eng* 26(2):211–224. <https://doi.org/10.1007/s10706-007-9158-z>
- Yoshida N (2015) Seismic ground response analysis. ISBN 13: 9789401794596, Springer, Dordrecht, 365pp.
- Yoshimine M, Nishizaki H, Amano K, Hosono Y (2006) Flow deformation of liquefied sand under constant shear load and its application to analysis of flow slide of infinite slope. *Soil Dyn Earthq Eng* 26(2–4):253–264. <https://doi.org/10.1016/j.soildyn.2005.02.016>
- Youd TL, Idriss IM (2001) Liquefaction resistance of soils: summary report from the 1996 NCEER and 1998 NCEER/NSF Workshops on evaluation of liquefaction resistance of Soils. *J Geotechn Geoenviron Eng Div ASCE* 127(4):297–313. [https://doi.org/10.1061/\(ASCE\)1090-0241\(2001\)127:10\(817\)](https://doi.org/10.1061/(ASCE)1090-0241(2001)127:10(817))
- Zhu J, Baise LG, Thompson EM (2017) An updated geospatial liquefaction model for global application. *Bull Seismol Soc Am* 107(3):1365–1385. <https://doi.org/10.1785/0120160198>

Publisher's Note Springer Nature remains neutral with regard to jurisdictional claims in published maps and institutional affiliations.

Springer Nature or its licensor (e.g. a society or other partner) holds exclusive rights to this article under a publishing agreement with the author(s) or other rightsholder(s); author self-archiving of the accepted manuscript version of this article is solely governed by the terms of such publishing agreement and applicable law.